ACTA PHYSIOLOGICA

Chronic adult-onset of growth hormone/IGF-I hypersecretion improves cognitive functions and LTP and promotes neuronal differentiation in adult rats

Journal:	*Acta Physiologica*
Manuscript ID	APH-2018-11-0656.R1
Manuscript Type:	Regular Paper
Date Submitted by the Author:	n/a
Complete List of Authors:	Martin-Rodriguez, Juan Francisco; Instituto de Biomedicina de Sevilla (IBiS), Hospital Universitario Virgen del Rocío/CSIC/Universidad de Sevilla, Laboratorio de Enfermedades Endocrinas Ramos-Herrero, Victor D.; Instituto de Biomedicina de Sevilla (IBiS), Hospital Universitario Virgen del Rocío/CSIC/Universidad de Sevilla, Laboratorio de Enfermedades Endocrinas; Universidad Pablo de Olavide, Division of Neurosciences Gutierrez-Parras, Gloria; Instituto de Biomedicina de Sevilla (IBiS), Hospital Universitario Virgen del Rocío/CSIC/Universidad de Sevilla, Laboratorio de Enfermedades Endocrinas; Universidad Pablo de Olavide, Division of Neurosciences Flores-Martinez, Alvaro; Instituto de Biomedicina de Sevilla (IBiS), Hospital Universitario Virgen del Rocío/CSIC/Universidad de Sevilla, Laboratorio de Enfermedades Endocrinas Madrazo-Atutxa, Ainara; Instituto de Biomedicina de Sevilla (IBiS), Hospital Universitario Virgen del Rocío/CSIC/Universidad de Sevilla, Laboratorio de Enfermedades Endocrinas Cano, David A.; Instituto de Biomedicina de Sevilla (IBiS), Hospital Universitario Virgen del Rocío/CSIC/Universidad de Sevilla, Laboratorio de Enfermedades Endocrinas Gruart, Agnès; Universidad Pablo de Olavide, Division of Neurosciences Delgado-García, José María; Universidad Pablo de Olavide, Division of Neurosciences Leal-Cerro, Alfonso; Instituto de Biomedicina de Sevilla (IBiS), Hospital Universitario Virgen del Rocío/CSIC/Universidad de Sevilla, Laboratorio de Enfermedades Endocrinas Leal-Campanario, Rocio; Universidad Pablo de Olavide Departamento de Fisiologia Anatomia y Biologia Celular, hysiology, Anatomy and Cell Biology
Key Words:	Growth Hormone, insulin-like growth factor type I, growth-hormone-secreting tumors, operant conditioning, LTP, passive avoidance, adult neurogenesis, rats

Acta Physiologica
Research article
Your ref.: APH-2018-11-0656

Number of words in the title: 18
Number of words in the Abstract: 200
Number of pages: 38
Number of figures: 8
Number of Tables: 1

Chronic adult-onset of growth hormone/IGF-I hypersecretion improves cognitive functions and LTP and promotes neuronal differentiation in adult rats

Juan Francisco Martín-Rodríguez[1], Víctor Darío Ramos-Herrero[1,2], Gloria G. Parras[1,2], Álvaro Flores-Martínez[1], Ainara Madrazo-Atutxa[1], David A. Cano[1], Agnès Gruart[2], José María Delgado-García[2], Alfonso Leal-Cerro[1*] and Rocío Leal-Campanario[2*].

[1]Instituto de Biomedicina de Sevilla (IBiS), Hospital Universitario Virgen del Rocío/CSIC/Universidad de Sevilla, Sevilla, Spain.

[2]Division of Neurosciences, University Pablo de Olavide, 41013 Seville, Spain

Short title: Effects of GH/IGF-I hypersecretion on the adult rat brain

Conflict of interest statement: Authors declare that there is no conflict of interest

***Corresponding authors:**

Rocío Leal-Campanario, Division of Neurosciences / Pablo de Olavide University / Ctra. de Utrera Km. 1 / 41013-Seville / Spain / E-mail: rleacam@upo.es / Phone: (+34) 954-977-427 / (+34) 686-945-207. And,

Alfonso Leal-Cerro, IBiS-Hospital Universitario Virgen del Rocío-CSIC-Universidad de Sevilla / 41013-Seville / Spain / E-mail: alealcerro@us.es / Phone: (+34) 955-923-051 / (+34) 649-448-668

Abstract

Aim

Besides their metabolic and endocrine functions, the growth hormone (GH) and its mediated factor, the insulin-like growth factor I (IGF-I), have been implicated in different brain functions, including neurogenesis. Long-lasting elevated GH and IGF-I levels result in non-reversible somatic, endocrine, and metabolic morbidities. However, the subcutaneous implantation of the GH-secreting (GH-S) GC cell line in rats leads to the controllable over-secretion of GH and elevated IGF-I levels, allowing the experimental study of their short-term effects on brain functions.

Methods

Adult rats were implanted with GC cells and checked 10 weeks later, when a GH/IGF-I-secreting tumor was already formed.

Results

Tumor-bearing rats acquired different operant conditioning tasks faster and better than controls and tumor-resected groups. They also presented better retentions of long-term memories in the passive avoidance test. Experimentally evoked long-term potentiation (LTP) in the hippocampus was also larger and longer-lasting in the tumor-bearing than in the other groups. Chronic adult-onset of GH/IGF-I hypersecretion caused an acceleration of early progenitors, facilitating a faster neural differentiation, maturation, and integration in the dentate gyrus, and increased the complexity of dendritic arbors and spine density of granule neurons.

Conclusion

Thus, adult-onset hypersecretion of GH/IGF-I improves neurocognitive functions, long-term memories, experimental LTP, and neural differentiation, migration, and maturation.

Key words: growth hormone, insulin-like growth factor type I, growth-hormone-secreting tumors, operant conditioning, LTP, neurogenesis, passive avoidance, rats

Abbreviations: bGH, bovine GH; BrdU, 5'-bromodeoxyuridine; DCX, doublecortin; fEPSP, field excitatory post-synaptic potential; GC, GH-S cell line; GH, growth hormone; GHR, GH receptors; GHRH, GH-releasing hormone; GH-S, GH-secreting; HFS, high-

frequency stimulation; hx, hypophysectomized; IGF-I, insulin-like growth factor type I; LTP, long-term potentiation; MCM2, minichromosome maintenance 2; NeuN, neuronal nuclear protein.

Introduction

GH is the most abundant hormone in the pituitary gland (1). Its secretion by somatotrophic cells is controlled by the hypothalamic GH-releasing hormone (GHRH) as stimulator and by somatostatin as inhibitor (2). Once released, GH travels to various target organs throughout peripheral tissues. Classically, the effect of GH includes hyperglycemia, lipolysis, and protein anabolism, and it has direct effects on cellular proliferation and differentiation.

IGF-I is the mediator factor of many of the actions of the GH. IGF-I is produced primarily in the liver, and in various tissues throughout the body. In response to GH (3), IGF-I regulates growth, glucose uptake, and protein metabolism (i.e., IGF-I-dependent GH effects). IGF-I-independent GH effects include stimulation of insulin secretion, lipolysis, and gluconeogenesis (4). GH can cross both the blood- (5) and CSF-brain barriers (6,7), as does the IGF-I (8).

The GH/IGF-I axis has been implicated in physiological brain functioning, neurogenesis, and myelination (9,10). Both GH and GH receptors (GHR) have been found in various brain regions of animals and humans (11), including choroid plexus, hypothalamus, cerebellum, thalamus, brain stem, hippocampus, striatum areas, and frontal cortex (12), suggesting that GH/IGF-I plays an important role in many different brain functions. GHR expression in the human hippocampus is greater than in other areas of the brain (6). This area is essential to learning, memory and higher cognitive functions (13), and synaptic plasticity (14,15).

Changes of the GH/IGF-I axis alter numerous cognitive functions, namely memory and executive functions (16). A drop in the secretion of GH has been associated with cognitive impairments in either physiological (17) or pathophysiological conditions (10,18), and is improved after a GH replacement therapy (19). In contrast, longer duration of GH hypersecretion and subsequent increase in IGF-I levels, as seen in untreated acromegaly, is associated with mild-to-moderate memory and executive function deficits (18,20), which are not improved in cured acromegalic patients (21). These results suggest that prolonged GH/IGF-I excess has long-term effects on brain functions (21).

Other roles of GH/IGF-I include inducing adult neurogenesis and increasing brain plasticity (14,15). GH increases hippocampal cell proliferation in adult hypophysectomized (hx) rats (22). Moreover, IGF-I also increases cell proliferation in hippocampal cells of hx rats which have low levels of circulating IGF-I (14,22). It has been shown that adult-onset deficiency in GH and IGF-I decreases survival of dentate granule neurons (23). GH seems to activate populations of resident stem and progenitor cells (24). At the same time, IGF-I also enhances neurogenesis (14,22,25) and help to rescue synaptic and motor deficits (26).

From an experimental point of view, the above-mentioned studies used transgenic, deficient, or pathophysiological animals, or were performed in culture. To our knowledge, no study had been carried out in an intact adult brain under hypersecretion of GH/IGF-I. Our study aims to analyze the putative effects of chronic GH/IGF-I hypersecretion in adult rats on instrumental learning —a function usually ascribed to prefrontal and related circuits (27, 28) —, LTP evoked in hippocampal CA3-CA1 synapses in behaving animals (29), and neurogenesis determined at the dentate nucleus (14,22). For this, we used Wistar Furth rats implanted with a GC cell line which resulted in the formation of solid, functional tumors (30,31). This animal model let us study the effects on associative learning, long-term memories, LTP, and neurogenesis of GH hypersecretion, as well as those following surgical resection of the tumor. Our results demonstrate that chronic (10 weeks) hypersecretion of GH/IGF-I enhances learning, memory, and synaptic plasticity in behaving intact adult animals. Moreover, hypersecretion of GH/IGF-I does not increase adult hippocampal neurogenesis, but promotes neuronal differentiation, migration, and maturation.

Results

Experimental groups. Animals included in this study were divided in three experimental groups. As illustrated in Figure 1a, animals in the control group were injected into the right flank with vehicle and did not develop a GH-S tumor. A second group of animals (the tumor-bearing group) was injected into the right flank with GC cells and developed a GH-S tumor. Finally, the tumor-resected group was injected into the right flank with GC cells and developed a tumor which was resected 8 weeks after the inoculation. The tumor-resected

group of animals was monitored daily after the removal of the tumor to make sure it did not reappear. As already reported (31) and further confirmed here, tumor-bearing rats increased their body weight significantly more than the other two groups (Figure 1b) and presented higher circulating levels of GH (Figure 1c) and IGF-I (Figure 1d). In addition, tumor resection in the tumor-resected group stopped the abnormal increase in animals' body weight (Figure 1b), and reverted GH (Figure 1c, blue bar A) and IGF-I (Figure 1d, blue bar A) levels to control values. Experimental tests were started 10 weeks after the injection of vehicle or GC cells (Figure 1a). Note that the levels of expression of GH (Figure 1c, blue bar B) and IGF-I (Figure 1d, blue bar B) in the tumor-resected group before the resecting surgery were like those presented by the tumor-bearing group (Figure 1c, gray bar B for GH and Figure 1d, gray bar B for IGF-I).

There was a fourth sham-surgery group in which we performed the same surgery to resect the tumor but in the opposite flank in order to find out if the surgery could affect the behavior of these animals. Results did not differ from the tumor-bearing group, this is the reason to discard this group from the study (data not shown).

Evaluation of motor activity and exploratory behavior. Animals included in the three experimental groups did not present significant differences in their locomotion and spontaneous exploratory activities, as evaluated in the open-field test (Figure 2). The absence of significant differences in the total activity measured for 15 min indicates that the presence of the GH/IGF-I hypersecretor tumor did not affect the locomotion and exploration of the animals, whose activity was like that of the other two groups [H = 1.559, with 2 degrees of freedom, $P = 0.459$; Kruskal-Wallis one-way ANOVA on ranks test].

Effect of GH/IGF-I hypersecretion on learning: instrumental conditioning task. To assess the effect of chronic hypersecretion of GH/IGF-I on learning capabilities of treated animals, we used two different operant conditioning tasks. It is established that wide areas of the cerebral cortex, including the prefrontal cortex and the hippocampus, and subcortical areas such as the striatum, participate in the acquisition and storage of this type of associative learning (28). In a first series of experiments, animals (n = 5 per group) were placed in Skinner boxes (Figure 3a) and shaped to press a lever to obtain a pellet of food. The shaping phase lasted for a maximum of 3 days. Once the target behavior was reached, rats had to perform a fixed-ratio (1:1) schedule ─ i.e., each lever press was reinforced with

a food pellet (Figure 3b, BL). Training sessions were performed daily and lasted for 15 min. The three groups of rats performed the fixed-ratio (1:1) schedule consistently, visiting the feeder and getting the pellet after each lever press with no significant differences between them [$F_{(2, 12)} = 0.047$; $P = 0.954$; two-way ANOVA repeated measures].

Animals were further trained for a fixed-ratio (FR 5:1) schedule for 5 days, in which they were reinforced with a pellet after pressing the lever 5 times. The three groups showed the same tendency to increase the number of lever presses across training [$F_{(2, 32)} = 30.925$; $P < 0.001$; two-way ANOVA repeated measures]. However, the total number of lever presses was different between the three groups [$F_{(2, 32)} = 30.925$; $P < 0.001$; two-way ANOVA repeated measures followed by pairwise Bonferroni test; Figure 3b]. Interestingly, the tumor-bearing group did not show significant differences in number of lever presses from the fixed-ratio (FR 1:1) schedule (84.2 ± 8.4) to the first FR 5:1 session (91.6 ± 4.2). However, the tumor-bearing group showed significant ($P \leq 0.04$) differences in the number of lever presses for all of the fixed-ratio (5:1) sessions as compared with the other two groups.

To elucidate whether the tumor-bearing group pressed the lever more times in the first conditioning session of the FR 5:1 schedule due to being more anxious rather than having learnt the task faster than the other two groups, animals were trained in a more complex paradigm. Now, animals were rewarded (again in a 5:1 fixed-ratio schedule) only during the period in which a small led light bulb, located over the lever, was switched on (Figure 3c). Lighted periods lasted for 20 s and were followed by non-lighted periods during which lever presses were not rewarded. There was no penalization if the animal pressed the lever during the dark period. As illustrated in Figure 3d, rats acquired this complex task steadily and progressively across the six training sessions [$F_{(10, 40)} = 0.717$; $P = 0.703$; two-way ANOVA repeated measures]. However, some statistically significant differences were found between groups [$F_{(2, 40)} = 4.769$; $P < 0.05$; two-way ANOVA repeated measures followed by pairwise Tukey test]. The tumor-bearing group always showed a "light on/off coefficient" above 0, meaning that these animals tended to press the lever more times with the light on than with the light off, and improved this coefficient across sessions ($P \leq 0.015$, for the first two sessions compared with the last two), indicating real learning of the task. The other two groups started the task with a coefficient below 0

and learnt from session 4 on (in the tumor-resected group, $P \leq 0.031$, for the first two sessions compared with the last two; in the control group, $P \leq 0.012$, for the first two sessions compared with the last two). In accordance, the tumor-bearing group learnt this task faster than the control (from session 3 to 5) and tumor-resected (session 3) groups, showing statistical differences ($P \leq 0.026$). These results indicate that the differences between the three groups found in the first session for the FR (5:1) schedule were due to adaptive learning strategies rather than to excessive anxiety levels

Overall, these results reliably demonstrated that chronic GH/IGF-I hypersecretion potentiates the proper acquisition of different types of operant conditioning task.

Effect of GH/IGF-I hypersecretion on memory: passive avoidance test. To evaluate if the chronic hypersecretion of GH/IGF-I could influence memory processes, the passive avoidance test was used (32). It is known that both amygdalar and hippocampal circuits are involved in this type of aversive memory (33). We determined the putative differences in the passive avoidance test for the three experimental groups by measuring the time taken by a rat to move from a white illuminated (aversive) to a black, dark (secure) compartment after the opening of a dividing door (Figure 4a). For the acquisition session, there was no significant difference between groups (n = 5 animals per group) in the time spent before entering the dark compartment (Figure 4b), where they received a mild shock. All animals presented low escape latencies: 8.72 ± 3.72 s for the control, 16.232 ± 2.07 s for the tumor-resected (blue bar), and 25.8 ± 7.87 s for the tumor-bearing (gray bar) animals, with no statistical differences between them ($P \geq 0.519$). In addition, three retention tests were carried out at 24 h, 72 h, and 1 week after the acquisition session. When the animals were placed back into the light chamber 24 h after receiving the foot shock, the latency to step-through was noticeably increased in the three groups without significant differences between them ($P = 0.167$), meaning that all animals remembered where they had received the foot shock (Figure 4b).

However, and as illustrated in Figure 4b, we found significant differences between the tumor-bearing group and the other two groups 72 h after the acquisition phase [$F_{(2,24)} = 24.764$; $P < 0.001$; two-way ANOVA repeated measures followed by the Tukey HSD test]. No differences in the consolidation phases (24 h, 72 h) were found between the control and the tumor-resected groups ($P = 0.277$).

To further evaluate long-term memory formation, we measured the escape latency 1 week after the acquisition phase (Figure 4b). Once again, we found significant differences in the latency to enter the dark compartment (where they had received the foot shock) between the tumor-bearing group and the control and tumor-resected groups ($P < 0.001$), which had no differences between them ($P = 0.073$).

Taken together, these results suggest that chronic hypersecretion of GH/IGF-I has a positive effect in the consolidation and retention of amygdalar and hippocampal-dependent memories.

Effect of GH/IGF-I hypersecretion on synaptic efficacy: in vivo LTP. We next studied LTP induced by high-frequency stimulation (HFS) of the CA3-CA1 synapse in alert behaving rats (Figure 5). LTP is a well-known form of synaptic plasticity that shares many properties with the functional synaptic potentiation evoked by the acquisition of new motor or cognitive abilities (29). To determine the putative effects of GH/IGF-I hypersecretion on synaptic plasticity, we induced LTP by HFS of the hippocampal Schaffer collateral pathway and compared the evolution of field excitatory post-synaptic potentials (fEPSPs) evoked at the CA3–CA1 synapse in freely moving rats (Figure 5). To obtain a baseline for evoked fEPSPs, animals were stimulated with single pulses for 15 min (at a rate of 3/min) at Schaffer collaterals (Figure 5c). For LTP induction, each animal received an HFS session (dotted line, Figure 5c). The effects of HFS were checked during the following 60 min, presenting the same stimulating pulses as during the baseline session. In addition, LTP evolution was checked for 30 min on the 3 days following the HFS session. With this protocol, LTP was induced in the three groups of animals [$F_{(2, 681)} = 4.74$; $P < 0.05$; two-way ANOVA repeated measures]. Interestingly, and comparing fEPSP amplitude values recorded during the 60 min following HFS, the tumor-bearing group presented a mean potentiation of 258.8 ± 30.8% (Figure 5c, gray squares) that was statistically higher than those presented by the tumor-resected (Figure 5c, blue squares) and control (Figure 5c, white squares) groups [$F_{(31, 681)} = 12.843$; $P < 0.001$; two-way ANOVA repeated measures followed by pairwise Fisher LSD test]. Experimentally evoked LTP remained larger in the tumor-bearing group than in the other two groups for the three days after the HFS session. Moreover, the tumor-resected group (Figure 5c, blue squares) presented LTP values like

those reached by the control group (Figure 5c, white squares), with no statistical differences between them.

Taken together, these results show that hypersecretion of GH/IGF-I enhances the activity-dependent synaptic potentiation taking place at the CA3-CA1 hippocampal synapse in conscious rats. LTP evoked in alert behaving rats by HFS of Schaffer collaterals further confirmed that hypersecretion of GH/IGF-I plays a definite positive role in maintaining long-term plastic changes at the hippocampal CA3-CA1 synapse, or at least that GH/IGF-I plays a role in this important memory-related hippocampal property.

Effect of the hypersecretion of GH/IGF-I on proliferation and differentiation of neural stem cells in the subgranular zone of the dentate gyrus. Neurogenesis in the adult dentate gyrus can be monitored by 5-bromo-2'-deoxyuridine (BrdU) incorporation into the nuclei of dividing cells. The nucleoside BrdU can label all S-phase cells in the adult dentate gyrus, regardless of the fate of these labeled cells; therefore, BrdU labeling is a general indicator for cell genesis in the brain. To evaluate neurogenesis, BrdU was injected daily for three consecutive days (50 mg/kg each; i.p.) to all rats ($n \leq 7$ per group). Animals were sacrificed 4 h after the last injection, time enough to evaluate cell proliferation (Figure 6a). At the same time, adult neurogenesis is a complex multi-stage process during which proliferating cells (e.g., proliferating stem cells), as well as their new-born progeny on their way to differentiating into neurons, express different proteins such as MCM2, which is a marker for proliferating cells, and DCX, which is a marker for immature neurons (34).

As shown in Figure 6c (top panels) we found no differences in the density of BrdU-positive cells between the three groups of animals [$F_{(2,9)} = 1.89$; $P = 0.206$; one-way ANOVA followed by the Tukey HSD test]. Although there was a slight decrease (40%) in the number of BrdU-positive cells for the tumor-bearing group in comparison with the control group, this decrease was not significantly different. Nevertheless, this result suggests that hypersecretion of GH/IGF-I does not increase the number of newly generated neurons compared with values collected from control and tumor-resected groups.

Different reports (35,36) have already indicated that substantial numbers of new cells are generated, but only a subset of them survives and differentiates into mature neurons within the dentate gyrus. Thus, to determine the effect of the hypersecretion of GH/IGF-I on neurogenesis, one has to combine this labeling with other immunohistological

markers that label newly formed neurons at later stages during the time-course of neurogenesis ─ i.e. proliferation and/or differentiation. Given that no changes were found in any of the three groups for BrdU, we postulated that the hypersecretion of GH/IGF-I might affect the pool of early differentiated neurons. To test this hypothesis, we examined the expression level of DCX, a microtubule-binding protein that regulates neuronal migration in pre- and postnatal development, as a marker of neuronal progenitors and early immature neurons (37). Notably, we observed that the DCX+ cell number was markedly increased in the tumor-bearing animals compared with the control group [$F_{(2, 18)} = 3.673$; $P = 0.038$; one-way ANOVA followed by Tukey test; Figure 6c, middle panels].

While DCX has been used in numerous studies as a hallmark for adult neurogenesis, the mere expression of DCX does not warrant the assumption that these DCX+ cells found are recently generated or migrating neuroblasts. If they are young migrating neuroblasts, there should be at least a small number of DCX+ cells capable of proliferating *in vivo*. We then estimated the numbers of maturing DCX+ granule cells co-expressing MCM2 (a protein essential for the pre-replication complex; 38). In this case, we found that the number of cells co- expressing MCM2/DCX was slightly higher in the tumor-bearing group as compared with the control or the tumor-resected animals, although there were non-significant ($P = 0.050$) differences between the three groups (Figure 6c, bottom panels).

In summary, taking all these results together we can posit that hypersecretion of GH/IGF-I might cause a premature acceleration of early progenitors toward neuronal differentiation (39).

Hypersecretion of GH/IGF-I accelerates the neurogenesis toward maturation and integration processes. To determine whether the new-born cells express a neuronal phenotype, we combined immunofluorescent labeling for BrdU and the neuronal marker NeuN (neuronal nuclear protein; 40) on sections from animals treated with BrdU for three consecutive days (150 mg/kg each) 3 weeks before they were killed. NeuN is the most widely used antibody marker of mature neurons, recently identified as Fox-3, an RNA-splicing regulator (41). In this case, the tumor-bearing group showed a significantly increased number of double-positive cells as compared with the control group (Figure 7b, top panel). Thus, the hypersecretion of GH/IGF-I enhanced the proportion of BrdU-positive cells in the granule layer that had differentiated into neurons, as indicated by the co-

expression of NeuN and BrdU [$t_{(6,\ 0.05)} = -5.3$; $P < 0.001$; Mann-Whitney U test]. Tumor-resected rats did not participate in this latter experiment since they did not show any significant difference with respect to the other two experimental groups in experiments illustrated in Figure 6.

We then examined the effect of the hypersecretion of GH/IGF-I on new-born neurons at a post-mitotic stage. To this end (see 42,43), we identified late immature and mature granule neurons using calretinin and calbindin combined with BrdU (Figures 7b, middle and bottom panels, respectively). Calretinin (Figure 7b, middle panels) has been described as a transient marker for immature granule neurons in mice (42), while calbindin (Figure 7b, bottom panels) is a calcium-binding protein commonly expressed by mature granule cells (43). Interestingly, we could not find any co-localization of BrdU+ cells with calretinin+ cells in any of the groups, but we found a notable increase of calbindin+ cells that co-localized with BrdU+ cells in the tumor-bearing group as compared with the control group [$t_{(4,\ 0.05)} = -3.99$; $P < 0.05$; T test].

In summary, we may state that hypersecretion of GH/IGF-I accelerates the intermediate phases of neurogenesis toward the maturation of new-born neurons into mature granule cells.

Hypersecretion of GH/IGF-/ affects the complexity of dendritic arbors and increases dendritic spine density on hippocampal granule neurons. To study the effects of the hypersecretion of GH/IGF-I on maturation of adult new-born cells, we three-dimensionally traced their dendritic arbors (Figure 8a) and made the corresponding Sholl analysis (44,45) to determine the number of intersections crossing equidistant concentric circles. The number of dendritic intersections (Figure 8b) in the circles ranging from 60 µm to 100 µm in the tumor-bearing group (gray squares) was significantly larger [$F_{(2,\ 195)} = 2.08$; $P \leq 0.05$, two-way ANOVA and Bonferroni corrected] than those presented by both tumor-resected and control groups (blue and white squares respectively).

We also found differences in the maximum dendritic length (Figure 8c) and in the total neurite length (Figure 8d) of DCX-positive granule cells in the dentate gyrus, which were increased in the tumor-bearing group as compared with control or tumor-resected animals [$F_{(2,\ 6)} = 18.653$; $P = 0.003$; Figure 8c. $F_{(2,\ 6)} = 10.94$; $P < 0.05$, Figure 8d; Krauskal-

Wallis test followed by pairwise Mann-Whitney test]. A Sholl analysis of the immature granule-cell dendrites showed that the hypersecretion of GH/IGF-I increases not only the intersection number of immature granule cells, but also the total and maximum dendritic lengths. To quantify the spine density in each experimental group, a Golgi-Cox staining was performed (Figure 8e and f). Results show that newly born neurons from the tumor-bearing group exhibit an increased dendritic spine number as compared with the other two groups [$F_{(2, 6)} = 8.276$; $P = 0.019$; one-way ANOVA followed by Tukey post hoc test]. In summary, all results illustrate that hypersecretion of GH/IGF-I produces considerably higher values for all parameters of the dendritic growth as well as an increased dendritic spine number as compared with the other two groups. These results illustrate the increase in complexity of new-born neurons in the dentate gyrus under GH/IGF-I hypersecretion.

Discussion

GH/IGF-1 has been involved in cognition, behavior, memory, and aging in humans and other mammals. The effects of long-term exposure to high levels of GH and IGF-I on cognitive performance have been established in humans, with evidence of moderate-to-severe memory impairments and decreased neural activity in specific brain areas in acromegaly patients (20). However, this disease typically follows an insidious clinical course spanning several years before being diagnosed. Given this slow development, clinical signs and symptoms of acromegaly often appear after a prolonged oversaturation of GH and IGF-I (46).

Acromegalic patients provide a clinical model for studying the noxious effects of supraphysiological GH and IGF-I levels in the brain and the subsequent effects on cognition processes across disease evolution. In contrast, animal transgenic models express the excess of GH from their embryonic development. In the present study, we were interested in comparing cognitive abilities in a non-genetically manipulated experimental animal where the GH excess was experimentally induced in adult ages (31). Using this model, our results show that chronic hypersecretion of GH/IGF-I in adult rats enhances cognitive functions such as learning and memory, potentiates synaptic plasticity determined by LTP induction, and accelerates the differentiation, migration, and maturation processes

of adult hippocampal neurogenesis *in vivo*. The particularities of this model, already described elsewhere (31), allows the study of the systemic effects of supraphysiological levels of GH/IGF-I in healthy adult mammals. Furthermore, the kinetic and tumor secretion dynamics of GC tumors allow the study of the insidious effect of this hypersecretion, which would differ from acute GH injection studies, being more comparable to pathophysiological situations similar to acromegaly.

The hippocampus is particularly involved in learning and memory processes (29,30), and synaptic plasticity is an essential subcellular mechanism underlying these two features. Here, we attempted to study how high levels of GH/IGF-I contribute to improve the acquisition of well-known hippocampal-dependent tasks—namely, the operant conditioning to determine associative learning capabilities, the passive avoidance test to measure memory, experimentally evoked LTP to measure synaptic plasticity, and dentate gyrus neurogenesis. Results clearly indicate a definite role of GH/IGF-I in the enhancement of different cognitive-related functions.

It has been shown that GH/IGF-I treatment improves cognitive function of GH-deficient young adults (47) and is also able to improve short- or long-term memory in rodents (48). At the same time, it seems that learning, on its own, enhances central IGF-I levels (49). Conversely, decreased GH secretion is associated with cognitive impairments, as shown in elderly men (17) and GH-deficient adult men (47). In the same way, a recent study has demonstrated the negative impact on learning and memory of increased GH activity in bovine GH (bGH) transgenic mice, while GH receptor antagonist (GHA) transgenic mice showed normal or even better learning capabilities (50).

The adult hippocampal neurogenesis contributes to various brain functions, such as learning and memory (51). The dentate gyrus, where adult-hippocampal neurogenesis takes place, is the principal input region of the intrinsic hippocampal circuit. Dentate granule cells receive excitatory inputs from the entorhinal cortex via the perforant pathway and send excitatory output to CA3 pyramidal neurons via the mossy fibers. Hilar mossy cells provide the first glutamatergic synapses to adult-born dentate granule cells ─ this functional interaction between granule cells and hilar mossy cells is a key component of the functions carried out by dentate neurons, including learning and memory processes (52). Experimental evidence suggest that new-born neurons integrate into the circuitry of the

adult dentate gyrus, making distinct contributions to the hippocampal function (53). Here, we have shown that hypersecretion of GH/IGF-I does not increase proliferation but accelerates the differentiation and synaptic integration processes into mature granule cells within the hippocampal dentate gyrus.

Learning-dependent changes in synaptic strength (which plays a critical role in memory formation) seem to regulate hippocampal neurogenesis by increasing proliferation and promoting survival of new-born granule neurons in the dentate gyrus (54). Adult-born neurons generated from a pool of precursor cells located in the subgranular zone of the dentate gyrus (55) are highly excitable and seem to participate in learning and memory formation (56). It has been shown that depletion of multipotent neural precursors by irradiation, antimitotic agents, or transgenic mouse models induces learning and memory deficits (57). Interestingly, GH treatment has been shown to promote proliferation and survival of subgranular zone neurospheres (58). Moreover, peripheral infusion of IGF-I induces neurogenesis in the adult hippocampus (14,22), while peripheral administration of bGH to adult intact rats stimulates neuronal proliferation (14). Our data not only support these findings but also show that hypersecretion of GH/IGF-I induces alterations in the dendritic morphology of the new-mature granule cells in the dentate gyrus by increasing branch number, dendritic length. and the spinogenesis of these cells. Overall, the functional effects described here for the chronic adult-onset of GH/IGF-I hypersecretion cannot be ascribed to side effects of the tumor, because the tumor-resected group did not present these cognitive, behavioral and neurogenetic improvements.

How do these results match with the cognitive decline seen in acromegalic patients and in transgenic male mice? Acromegaly is a rare but severe hormonal disorder resulting from aberrant GH secretion and subsequent increase of IGF-I, usually due to a pituitary adenoma that develops insidiously and progressively for years. In addition to systemic complications and cognitive impairments, structural alterations in gray and white brain matter (including the hippocampus) in acromegaly patients have been reported (59). However, the increase in hippocampal volume observed in these patients seems not to be related to increased neurogenesis in hippocampus (59), but to increased gliogenesis and glial activity related to myelin production (60). Our results are in apparent contradiction with cognitive studies performed in acromegalic patients, including some published by our

group (18, 20, 21). Our study reveals a different outcome of the effect of hypersecretion of GH/IGF-I on learning, memory, and synaptic plasticity, probably because in acromegaly from 6 to 10 years of hormone excess elapse until clinical signs or symptoms are detected and lead to the diagnostic work-up and treatment (61). Our results might indicate that the beneficial effects of high GH and IGF-I levels could be extended to several weeks of exposure chronic, at least in rats. An excess of GH / IGF-I signaling over a longer period of time will have deleterious effects on the structure and function of the CNS, as documented in humans with acromegaly (20, 59). In this regard, it has recently been shown that twelve-month-old male bGH mice displayed significantly poorer learning and suppressed memory retention when compared with the corresponding wild-type group (50). In that study, bGH mice were over exposed to GH for 12 months while in our model rats were exposed to GH for only 10 weeks. According to the present results, not only is the amount of available GH/IGF-I different, but also the time to GH exposure should be taken into consideration. Indeed, in bGH mice, as well as in acromegalic patients, the over-exposure to high levels of GH/IGF-I lasts so long that possibly the pool of neurogenic stem cells depletes completely, leading to reduced neuron renewal and the subsequent decline in cognitive functions. Something similar might happen during aging, when cognitive functions also decline, but in this case GH/IGF-I levels decrease with time, impeding neurogenesis and the formation of new neurons.

Taken together, these findings highlight the potential therapeutic role of stimulating neurogenesis to enhance cognitive functions and a potential role of GH in modulating memory, cognition, behavior, and neurogenesis in normal and abnormal GH states.

Methods

Experimental animals. Female adult Wistar Furth rats used in this study were purchased from an official supplier (Charles River Laboratories, L'Arbresle, France) and maintained at the Animal Facilities of the University Pablo de Olavide (Seville, Spain). Upon their arrival, animals were placed in individual cages and weighed daily across the whole experiment. They were maintained at room temperature (20–22 °C) and were

exposed daily to a 12-hour light/12-hour dark cycle. In addition, they had free access to both water and, unless otherwise stated, food.

All procedures involving experimental animals were performed in accordance with Spanish (BOE 34/11370-421, 2013) and European (2010/63/EU) guidelines for animal welfare and handling in chronic experiments. All experimental protocols were also approved by the local Ethics Committee of the University Pablo de Olavide.

Graft induction and surgery. Somatotroph/GH-S adenomas/tumors were generated by subcutaneous injection of 1×10^7 GC cells (dissolved in 0.3 mL of PBS) in the right flank of 7-week-old rats. GC-cell-culture conditions, molecular characteristics, and metabolism of GH tumors have been described elsewhere (30, 31). Control animals were injected with the same volume of PBS and with the same time schedule. After the injection, rats were kept in their home cages for 2 weeks under standard conditions. At this point, tumor presence was checked and rats without clear evidence of a tumor were eliminated.

Tumor surgery included tumor removal and blood sampling from the subclavian vein. Rats were anesthetized with ketamine hydrochloride (40 mg/kg; i.p.) plus xylazine (8 mg/kg; i.m.). Additionally, sham surgery was performed in another two groups by making an incision on the same (control) or on the contralateral (tumor-bearing) side of the tumor. The tumor-resected group was monitored every day after the removal surgery to make sure there was no reappearance of the tumor, in which case (less than 0.5% of the sham surgeries) the animal was eliminated. The surgery for resection of the tumor with no reappearance had an efficacy of 98%.

Hormone measurements. For *in vivo* hormone measurements, blood from the subclavian vein was collected in the morning and centrifuged to obtain serum. GH and IGF-1 levels were measured by ELISA commercial kits (EZRMGH-45K, Merck Millipore, Madrid, Spain; and AC-18F1, Immunodiagnostic Systems, Boldon, Tyne & Wear, UK) in accordance with the manufacturer's protocol.

Spontaneous locomotion and activity in the open field. To evaluate spontaneous locomotor and exploratory activities, rats (n = 7 control; n = 5 tumor-resected; n = 12 tumor-bearing) were placed for 15 min in an activity-recording cage (54 × 50 × 37 cm; Ugo Basile, Monvalle, Italy). This apparatus consisted of a transparent walled platform

containing horizontal and vertical infrared sensors coupled to a counter that totals photocell disruptions. The number of photocell disruptions, for the 15-minute observation period, was computed and stored (total activity / 15 min; see Figure 2).

Operant conditioning procedures. Training and testing took place in five Skinner box modules measuring 29.2 × 24.1 × 21 cm (MED Associates, St. Albans, VT, USA). Each operant chamber was housed within a sound-attenuating chamber (90 × 55 × 60 cm), which was constantly illuminated (19 W lamp) and exposed to a 45-dB white noise (Cibertec, S.A., Madrid, Spain). Each Skinner box was equipped with a food dispenser from which pellets (Noyes formula P; 45 mg; Sandown Scientific, Hampton, UK) could be delivered by pressing a lever located nearby. Before training, rats (n = 5 per group) were handled daily for 7 days and food-deprived to 80–85% of their free feeding weight. Shaping took place for 15 min on each of 3 consecutive days, in which rats were shaped to press the lever to receive pellets from the food tray, using a fixed ratio (FR 1:1) schedule. Conditioning was carried out for 5 days, using a fixed ratio 5:1 (FR 5:1) schedule (Figure 3a). The start and end of each session was indicated by a tone (2 kHz, 200 ms, 70 dB) provided by the loudspeaker located in the recording chamber.

After 5 days following the 5:1 schedule, additional operant training was performed with the same three groups of animals for 6 days using an FR 5:1 light/dark protocol (Figure 3c). For this purpose, each Skinner box was provided with a small house light (3 W) mounted over the lever. In this protocol, only lever presses performed by the experimental animal during the lighted period (20 s) were reinforced with a pellet. Lever presses performed during the dark protocol (20 ± 10 s) were not reinforced. Animals were not penalized if lever presses were performed during the dark period. A light on/off coefficient (Figure 3d) was calculated as follows: (No. of lever presses with light – No. of lever presses with light off) /total No. of lever presses.

Conditioning programs, lever presses and delivered reinforcements were monitored and recorded by a computer, using a MED-PC program (MED Associates).

Passive avoidance test. Passive avoidance is a fear-motivated test classically used to assess short-term and long-term memories in small laboratory animals (32,33). We used a standard passive avoidance step-through apparatus (57 × 27 × 30 cm; Ugo Basile) with the

three groups of experimental animals. The conditioning chamber had two compartments (light and dark) with the same dimensions, and a sliding door separating them. The sides and top of the apparatus were made of Plexiglas and the floor comprised stainless-steel bars (2.5 mm in diameter) placed at intervals of 1 cm, through which a mild foot shock could be applied (100 Hz, 3 s, 0.8 mA). The lit (start) compartment was white and illuminated by a light fixture (3 LED, white-light), while the dark (escape) compartment was black and not illuminated at all. The experimental room was dimly illuminated, and a 68-dB white noise generated from an office computer (AnyMaze software, Stoelting, Wood Dale, IL, USA) was used to mask any background noise. The apparatus was cleaned with a 70% ethanol solution prior to the training and testing of each animal.

Experimental animals (n = 5 per group) were habituated to the apparatus for 5 min prior to testing. Each animal was gently placed in the lit compartment for 30 s, after which the guillotine door was lifted. The latency with which the animal crossed to the dark (shock) compartment was recorded. Once the animal had crossed over with all four paws in the dark compartment, the door was closed, and a foot shock was delivered. After 5 s, the rat was removed from the apparatus and placed back into its home cage.

Retention sessions were carried out as follows. The rat was retested in the same way as before at 24 h, 72 h, or 1 week after the acquisition (baseline) test. The latency to enter the dark compartment was recorded for up to 300 s. During retention sessions, no electric shock was applied. Good retention performance was indicated by high latency scores while poor retention was evidenced by low scores of latencies to go into the black, dark side of the apparatus.

Long-term potentiation. Following previous descriptions from our group (29), LTP was evoked and recorded in alert behaving rats. For this, animals (n = 12 per group) were anesthetized with 4% chloral hydrate at a dose of 1 mL/100 g body weight. Once anesthetized, they were implanted with bipolar stimulating electrodes in the right Schaffer collateral/commissural pathway of the dorsal hippocampus (3.5 mm lateral, 3.2 mm posterior to Bregma, and 3.2 mm from the brain surface; 62) and with recording tetrodes aimed at the ipsilateral stratum radiatum underneath the CA1 area (2.5 mm lateral, 3.6 mm posterior to Bregma, and 2.6 mm from the brain surface; 62). Stimulating and recording electrodes were made from 25 μm, Teflon-coated tungsten wire (Advent Research

Materials Ltd., Oxford, UK). Electrodes were surgically implanted in the CA1 area using as a guide the field potential depth profile evoked by paired (40 ms of interval) pulses presented to the ipsilateral Schaffer collateral pathway. Recording electrodes were fixed at the site where a reliable monosynaptic fEPSP was recorded. A 0.1 mm bare silver wire was affixed to the bone as ground. Implanted wires were connected to two separate 4-pin sockets (RS-Amidata, Madrid, Spain). Sockets were fixed to the skull with the help of two small screws and dental cement (29).

For LTP induction, animals were placed in a small box located inside a larger Faraday cage. All *in vivo* recordings were carried out in awake, non-anesthetized animals one week after the electrode implantation surgery. For each animal, the stimulus intensity was set well below the threshold for evoking a population spike ─ usually 30–40% of the intensity necessary for evoking a maximum fEPSP response. Recordings were carried out using Grass P511 differential amplifiers with a bandwidth of 0.1 Hz–10 kHz (Grass-Telefactor, Middleton, WI, USA). Synaptic field potentials in the CA1 area were evoked by single, 100 μs, square, biphasic (negative-positive) pulses applied to Schaffer collaterals.

For evoking LTP, an HFS protocol was used. Each animal was presented with five 200 Hz, 100 ms trains of pulses at a rate of 1/s. These trains were presented six times in total, at intervals of 1 min. The 100 μs, square, biphasic pulses used to evoke LTP were applied at the same intensity used for evoking baseline records. Baseline records were collected for 15 min with the evoking stimuli presented every 20 s. After the HFS protocol, fEPSPs were recorded again for 1 h. Additional recordings were carried out for 30 min on each of the 3 following days (Figure 5c).

BrdU injections. Two separate experiments were conducted to assess the effect of GH/IGF-I hypersecretion on cell proliferation and new-born cell survival in the dentate gyrus of the adult rat. A published protocol was followed for the preparation, preservation, and injection of the BrdU solution (63). This solution was freshly prepared daily. For the first experiment, 18-week-old rats (control group, n = 8; tumor-resected, n = 6; tumor-bearing, n = 8) received a daily injection (i.p.) of BrdU for three consecutive days (50 mg/kg each) and were sacrificed 4 h after the last injection. For the second experiment, 15-week-old rats (n = 4 per group) also received a daily single injection (i.p.) of BrdU on three

consecutive days (150 mg/kg each) and were sacrificed 21 days after the first injection. Tumor-resected rats did not participate in this latter experiment.

Molecular markers. To define the cells at specific stages of adult hippocampal neurogenesis, we used the following molecular markers: doublecortin (DCX) to label neural progenitors and immature granule cells (34,37), minichromosome maintenance 2 (MCM2) to label early and late early transit amplifying progenitors (37,38), neuronal nuclei (NeuN) to label immature and mature granule cells (40), calretinin to label postmitotic immature granule cells (42), and calbindin to label mature granule cell (37,43). Primary antibodies used are indicated in Table 1.

Tissue preparation and immunohistochemistry. Rats were sacrificed with a lethal dose of thiobarbital (Braun Medical, S.A., Barcelona, Spain) and perfused transcardially with ice-cold saline solution and 4% PFA (wt/vol) in PBS. Brains were then fixed in 4% PFA at 4 ºC overnight and embedded in 30% sucrose solution in PBS until they sank. Then, brains were embedded in OCT compound (Tissue-Tek, Sakura Finetek USA). Coronal sections (40 µm thick) were obtained into a cryostat and preserved at -20 ºC in cryoprotective solution (30% ethylene glycol, 30% glycerol, 30% dH2O, and 10% 10x PBS) for immunohistochemical and immunofluorescence analysis.

Immunohistochemistry and immunofluorescence analyses were performed as described previously (43,44). Briefly, free-floating sections were rinsed three times in PBS. Antigen retrieval was performed with 80 ºC boiling 0.1M sodium citrate buffer, pH 6. For doublecortin (DCX) labeling, an 80 ºC boiling TRIS-EDTA buffer, pH 9, was used for the antigen retrieval. For BrdU labeling, prior to immunohistochemistry, DNA was denaturalized with 2N HCl 30 min at 37 ºC and neutralized with 0.1M borate buffer, pH 8.5. For immunohistochemical staining, sections were quenched with 3% hydrogen peroxide. After primary antibody incubation (Table 1), the sections were washed and incubated with the appropriate biotinylated secondary antibody (Vector Laboratories, Burlingame, CA, USA), or with the appropriate (Alexa Fluor 488 for MCM2, NeuN, calretinin, and calbindin or 568 for DCX and BrdU) conjugated secondary antibody. Staining for diaminobenzidine (DAB) was performed with the ABC Elite immunoperoxidase system (Vector Laboratories). The blocking, primary antibody, and secondary antibody incubations were performed using PBS + TRITON 100 (0.2%) as

diluent with 10% normal donkey serum. A minimum of three washes with PBS + TRITON 100 (0.2%) was completed between steps. For light microscopy, after DAB precipitation, DNA counterstaining was performed using Mayer's hematoxylin (Bio Optica), and the section were dehydrated and mounted with DPX. After immunofluorescence labeling, nuclei were visualized by DAPI staining and the sections were mounted with DAKO fluorescent mounting medium.

Quantification and image analysis. The quantification of antigen-positive cells (DCX, BrdU) was performed counting all the positive cells in the subgranular layer of the dentate gyrus after DAB immunohistochemistry. Sections were analyzed with an Olympus BX61 microscope associated to the new Computer Assisted Stereological Toolbox (newCAST™) by Visiopharm, coupled to an Olympus DP72 microscope camera (Olympus, Tokyo, Japan). Measurements of the rat dentate gyrus area were obtained with the software VIS™ by Visiopharm. Quantifications were performed with the help of the Cell Counter tool. Data were represented as number of positive cells per mm^2 (n = 4–8 rats/group, n = 6 sections/rat, 480 µm between each section). The number of double-positive cells (DCX/MCM2, BrdU/NeuN, BrdU/calretinin and BrdU/calbindin) in the same area was counted after double immunofluorescence. The sections were visualized on a ZEISS LSM-7 DUO confocal system, and all the double-positive cells were counted with the software ZEN 2012 (Carl Zeiss, Oberkochen, Germany). Results were represented as number of double-positive cells per section (n = 3-4 rats/group, n= 6 sections/rat, 480 µm between each section).

Sholl analysis. To compare the dendritic growth and complexity of newly born neurons between groups, we performed morphological analysis of the DCX+ dendritic trees using the Neurolucida neuron-tracing system (MBF Bioscience, Williston, VT, USA) on an Olympus microscope (BX61; Olympus). Only the DCX+ neurons that exhibited the following features were chosen for this analysis: i) vertically oriented dendrites reaching the molecular layer; ii) at least one second-order dendrite; iii) no truncated branches near the soma; and, iv) absence of overlap with dendrites of neighboring neurons (64). Five such neurons were selected from each animal belonging to the three groups (n = 3 animals per group; n = 15 neurons per group) and were traced at 40× magnification using the

Neurolucida neuron-tracing system. The complexity of the dendritic arbors was assessed using Sholl analysis to determine the number of dendritic intersections crossing equidistant concentric circles. Data accounting for other morphological measurements, such as the total dendritic length and maximum dendritic length, were also measured and compared.

Golgi-Cox staining. To examine changes in spine density, we performed a modified Golgi-Cox staining method (65). Briefly, 50-µm free-floating pre-fixed sections were rinsed three times in TBS-TX100 0.1% (TBS + TRITON 100; 0.1%). Then, sections were immersed in a Golgi-Cox solution for 14 days, changing solutions daily. Sections were mounted onto Superfrost® Plus slides (Thermo Fisher Scientific, Waltham, MA USA), using gelatin 2% as flotation medium. Once dried in the dark, they were incubated with ammonium hydroxide 20% for 10 min. Finally, dehydrated slides were coverslipped with DPX. Z-stack bright-field images were acquired every 0.5 µm z-distance using a BX-61 microscope (Olympus) at a 100× magnification, and with a resolution of 2070×1548 pixels. Quantification of dendritic spines in the hippocampal region was performed by averaging ≥ 12 dendritic segments (50 µm) from different neurons per animal (n = 3 animals in each experimental cohort) using ImageJ software (NIH, Bethesda, MA, USA). Only dendritic segments ≥ 50 µm away from the cell body were included in the analysis.

Statistical analysis. Collected results are represented as mean ± SEM. A $P < 0.05$ was considered significant. No statistical methods were used to predetermine sample sizes, but the sample size of $n \geq 4$ was justified by the cumulated experience from previous studies employed in the field. Prior to the statistical analysis, data was analyzed with the Shapiro-Wilk normality test and the homogeneity of the variance was analyzed with the Levene test. For comparison of two independent groups (Figure 7), Mann–Whitney–Wilcoxon test (with non-normal distribution) was performed. For multiple comparisons (Figures 2, 6 and 8), data with a normal distribution were analyzed by one-way-ANOVA. Statistical significance of non-parametric data for multiple comparisons was determined by Kruskal–Wallis one-way ANOVA followed by pairwise Mann–Whitney test. To compare dependent measurements (Figures 1, 3-5), we used the two-way repeated measures ANOVA. Given that the number of hypotheses tested across the study and the number multiple comparisons that each experiment involved (especially, behavioral and

electrophysiological experiments) were large, thus producing a substantial inflation of Type-1 error, we opted to use FDR-controlling procedures (Hochberg–Benjamini correction) for multiplicity (66) at the ANOVA level to control for multiple hypothesis testing. This was conducted aiming at increasing our power at the cost of increasing the rate of type-1 error. Tukey's method was then applied at the level of post-hoc tests with the aim of controlling FWER. Statistics were performed with the help of the Sigma Plot 11 program. All data were processed randomly and blinded.

Author contributions

Author contributions: AG, AL-C, DAC, JFM-R, JMD-G, RL-C designed research; AF-M, GGP, JFM-R, AG, RL-C, VDR-H performed research; AF-M, AM-A, GGP, JFM-R, RL-C, VDR-H analyzed data; AG, AL-C, JFM-R, JMD-G, RL-C wrote the paper. All the authors revised the final version of the manuscript.

Acknowledgements

This study was supported by a grant from the Junta de Andalucía (PI-0302-2012) to RL-C and by grants from the Spanish Ministry of Economy and Competitiveness (BFU2014-56692-R and BFU2017-82375-R) and the Junta de Andalucía (BIO122) to AG and JMD-G, and grants from the ISCIII-*Subdirección General de Evaluación y Fomento de la Investigación* co-funded with *Fondos* FEDER (PI16/00175) and the Nicolás Monardes program of the Andalusian Ministry of Health (C-0015-2014) to DAC. Authors thank Mr. Roger Churchill for his help in manuscript editing.

References

1. Melmed S (2016) New therapeutic agents for acromegaly. Nat Rev Endocrinol 12(2):90-98. doi: 10.1038/nrendo.2015.196.
2. Morishita M, Iwasaki Y, Onishi A, Asai M, Mutsuga N, Yoshida M, Oiso Y, Inoue K, Murohara T (2003) The effects of GH-releasing hormone/somatostatin on the 5'-promoter activity of the GH gene in vitro. J Mol Endocrinol. 31(3):441-448.
3. Bikle DD, Tahimic C, Chang W, Wang Y, Philippou A, Barton ER (2015) Role of IGF-I signaling in muscle bone interactions. Bone 80:79-88. doi: 10.1016/j.bone.2015.04.036.
4. Dominici FP, Argentino DP, Muñoz MC, Miquet JG, Sotelo AI, Turyn D (2005) Influence of the crosstalk between growth hormone and insulin signalling on the modulation of insulin sensitivity. Growth Horm IGF Res 15(5):324-336. doi: 10.1016/j.ghir.2005.07.001.
5. Pan W, Yu Y, Cain CM, Nyberg F, Couraud PO, Kastin AJ (2005) Permeation of growth hormone across the blood-brain barrier. Endocrinology 46(11):4898-4904. doi: 10.1210/en.2005-0587.
6. Lai ZN, Emtner M, Roos P, Nyberg F (1991) Characterization of putative growth hormone receptors in human choroid plexus. Brain Res 546(2):222-226. doi: 10.1016/0006-8993(91)91485-J.
7. Johansson JO, Larson G, Andersson M, Elmgren A, Hynsjö L, Lindahl A, Lundberg PA, Isaksson OGP, Lindstedt S: Bengtsson BÅ (1995) Treatment of growth hormone-deficient adults with recombinant human growth hormone increases the concentration of growth hormone in the cerebrospinal fluid and affects neurotransmitters. Neuroendocrinology 61(1):57-66. doi: 10.1159/000126813.
8. Carro E, Spuch C, Trejo JL, Antequera D, Torres-Aleman I (2005) Choroid plexus megalin is involved in neuroprotection by serum insulin-like growth factor I. J Neurosci 25(47):10884-10893. doi: 10.1523/JNEUROSCI.2909-05.2005.
9. O'Kusky JR, Ye P, D'Ercole AJ (2000) Insulin-like growth factor-I promotes neurogenesis and synaptogenesis in the hippocampal dentate gyrus during postnatal development. J Neurosci 20(22):8435-8442.

10. Nyberg F, Hallberg M (2013) Growth hormone and cognitive function. Nat Rev Endocrinol 9(6):357-365. doi: 10.1038/nrendo.2013.78.
11. Nyberg F (2000) Growth hormone in the brain: characteristics of specific brain targets for the hormone and their functional significance. Front Neuroendocrinol 21:330-348. doi: 10.1006/frne.2000.0200.
12. Chung YH, Shin CM, Joo KM, Kim MJ, Cha CI (2002) Region-specific alterations in insulin-like growth factor receptor type I in the cerebral cortex and hippocampus of aged rats. Brain Res 946(2):307–313. doi: 10.1016/S0006-8993(02)03041-X.
13. van Dam PS, Aleman A (2004) Insulin-like growth factor-I, cognition and brain aging. Eur J Pharmacol 490(1-3):87-95. doi: 10.1016/j.ejphar.2004.02.047.
14. Åberg ND (2010) Role of the growth hormone/insulin-like growth factor 1 axis in neurogenesis. Endocr Dev 17:63-76. doi: 10.1159/000262529.
15. Malek M, Sarkaki A, Zahedi-Asl S, Rajaei Z, Farbood Y (2017) Effect of intra-hippocampal injection of human recombinant growth hormone on synaptic plasticity in the nucleus basalis magnocellularis-lesioned aged rats. Arq Neuropsiquiatr 75(7):477-483. doi: 10.1590/0004-282X20170074.
16. 16-Falleti MG, Maruff P, Burman P, Harris A (2006) The effects of growth hormone (GH) deficiency and GH replacement on cognitive performance in adults: a meta-analysis of the current literature. Psychoneuroendocrinology 31(6):681-691. doi: 10.1016/j.psyneuen.2006.01.005.
17. Aleman A, de Vries WR, de Haan EHF, Verhaar HJJ, Samson MM, Koppeschaar HPF (2000) Age-sensitive cognitive function, growth hormone and insulin-like growth factor 1 plasma levels in healthy older men. Neuropsychobiology 41:73-78. doi: 10.1159/000026636.
18. Tanriverdi F, Yapislar H, Karaca Z, Unluhizarci K, Suer C, Kelestimur F (2009) Evaluation of cognitive performance by using P300 auditory event related potentials (ERPs) in patients with growth hormone (GH) deficiency and acromegaly. Growth Horm IGF Res. 19(1):24–30. doi: 10.1016/j.ghir.2008.05.002.
19. Arwert, LI, Veltman, DJ, Deijen, JB, van Dam, PS, Drent ML (2006) Effects of growth hormone substitution therapy on cognitive functioning in growth hormone

deficient patients: a functional MRI study. Neuroendocrinology 83(1):12-19. doi: 10.1159/000093337.

20. Leon-Carrion J, Martín-Rodriguez JF, Madrazo-Atutxa A, Soto-Moreno A, Venegas-Moreno E, Torres-Vela E, Benito-López P, Gálvez MA, Tinahones FJ, Leal-Cerro A. (2010) Evidence of cognitive and neurophysiological impairment in patients with untreated naïve acromegaly. J Clin Endocrinol Metab 95(9):4367–4379. doi: 10.1210/jc.2010-0394.
21. Martín-Rodriguez JF, Madrazo-Atutxa A, Venegas-Moreno E, Benito-López P, Gálvez MÁ, Cano DA, Tinahones FJ, Torres-Vela E, Soto-Moreno A, Leal-Cerro A (2013) Neurocognitive function in acromegaly after surgical resection of GH-secreting adenoma versus naïve acromegaly. PLoS One 8(4):e60041. doi: 10.1371/journal.pone.0060041.
22. Åberg ND, Johansson I, Åberg MA, Lind J, Johansson UE, Cooper-Kuhn CM, Kuhn HG, Isgaard J (2009) Peripheral administration of GH induces cell proliferation in the brain of adult hypophysectomized rats. J Endocrinol 201(1):141-150. doi: 10.1677/JOE-08-0495.
23. Lichtenwalner RJ, Forbes ME, Sonntag WE, Riddle DR (2006) Adult-onset deficiency in growth hormone and insulin-like growth factor-I decreases survival of dentate granule neurons: insights into the regulation of adult hippocampal neurogenesis. J Neurosci Res. 83(2):199-210. doi: 10.1002/jnr.20719.
24. Blackmore DG, Reynolds BA, Golmohammadi MG, Large B, Aguilar RM, Haro L, Waters MJ, Rietze RL (2012) Growth hormone responsive neural precursor cells reside within the adult mammalian brain. Sci Rep 2:250. doi: 10.1038/srep00250.
25. Trejo JL, Carro E, Torres-Alemán I (2001). Circulating insulin-like growth factor I mediates exercise-induced increases in the number of new neurons in the adult hippocampus. J Neurosci 21(5):1628-1634.
26. Bozdagi O, Tavassoli T, Buxbaum JD (2013) Insulin-like growth factor-1 rescues synaptic and motor deficits in a mouse model of autism and developmental delay. Mol Autism. 4(1):9. doi: 10.1186/2040-2392-4-9.
27. Jurado-Parras MT, Gruart A, Delgado-García JM (2012) Observational learning in mice can be prevented by medial prefrontal cortex stimulation and enhanced by

nucleus accumbens stimulation. Learn Mem. 19(3):99-106. doi: 10.1101/lm.024760.111.

28. Jurado-Parras MT, Sánchez-Campusano R, Castellanos NP, del-Pozo F, Gruart A, Delgado-García JM. (2013) Differential contribution of hippocampal circuits to appetitive and consummatory behaviors during operant conditioning of behaving mice. J Neurosci. 33(6):2293-2304. doi: 10.1523/JNEUROSCI.1013-12.2013.
29. Gruart A, Muñoz MD, Delgado-García JM (2006) Involvement of the CA3-CA1 synapse in the acquisition of associative learning in behaving mice. J Neurosci 26(4):1077-1087. doi: 10.1523/JNEUROSCI.2834-05.2006.
30. Timsit J, Riou B, Bertherat J, Wisnewsky C, Kato NS, Weisberg AS, Lubetzki J, Lecarpentier Y, Winegrad S, Mercadier JJ (1990) Effects of chronic growth hormone hypersecretion on intrinsic contractility, energetics, isomyosin pattern, and myosin adenosine triphosphatase activity of rat left ventricle. J Clin Invest 86(2):507-515. doi: 10.1172/JCI114737.
31. Martín-Rodríguez JF, Muñoz-Bravo JL, Ibañez-Costa A, Fernandez-Maza L, Balcerzyk M, Leal-Campanario R, Luque RM, Castaño JP, Venegas-Moreno E, Soto-Moreno A, Leal-Cerro A, Cano DA (2015) Molecular characterization of growth hormone-producing tumors in the GC rat model of acromegaly. Sci Rep 5:16298. doi: 10.1038/srep16298.
32. Myhrer T (2003) Neurotransmitter systems involved in learning and memory in the rat: a meta-analysis based on studies of four behavioral tasks. Brain Res Brain Res Rev 41(2-3): 268-287. doi: 10.1016/S0161-813X(03)00040-8.
33. Redondo RL, Kim J, Arons AL, Ramirez S, Liu X, Tonegawa S (2014) Bidirectional switch of the valence associated with a hippocampal contextual memory engram. Nature 513(7518):426-430. doi: 10.1038/nature13725.
34. von Bohlen und Halbach O (2011) Immunohistological markers for proliferative events, gliogenesis, and neurogenesis within the adult hippocampus. Cell Tissue Res. 345(1):1-19. doi: 10.1007/s00441-011-1196-4.
35. Cameron HA, McKay RD (2001) Adult neurogenesis produces a large pool of new granule cells in the dentate gyrus. J Comp Neurol 435(4):406-417. doi: 10.1002/cne.1040.

36. Sun W, Winseck A, Vinsant S, Park O, Kim H, Oppenheim RW (2004) Programmed cell death of adult-generated hippocampal neurons is mediated by the proapoptotic gene Bax. J Neurosci, 24:11205-11213. doi: 10.1523/JNEUROSCI.1436-04.2004.
37. Osman AM, Porritt MJ, Nilsson M, Kuhn HG (2011) Long-term stimulation of neural progenitor cell migration after cortical ischemia in mice. Stroke 42:3559-3565. doi: 10.1161/STROKEAHA.111.627802.
38. Tye BK (1999) Minichromosome maintenance as a genetic assay for defects in DNA replication. Methods 18(3):329-334. doi: 10.1006/meth.1999.0793.
39. Amador-Arjona A, Cimadamore F, Huang CT, Wright R, Lewis S, Gage FH, Terskikh AV (2015) SOX2 primes the epigenetic landscape in neural precursors enabling proper gene activation during hippocampal neurogenesis. Proc Natl Acad Sci U S A 112(15): E1936 -E1945. doi: 10.1073/pnas.1421480112.
40. Mullen RJ, Buck CR, Smith AM (1992) NeuN, a neuronal specific nuclear protein in vertebrates. Development 116(1):201-211.
41. Kim KK, Adelstein RS, Kawamoto S (2009) Identification of neuronal nuclei (NeuN) as Fox-3, a new member of the Fox-1 gene family of splicing factors. J Biol Chem 284(45):31052-31061. doi: 10.1074/jbc.M109.052969.
42. Brandt MD, Jessberger S, Steiner B, Kronenberg G, Reuter K, Bick-Sander A, von der Behrens W, Kempermann G (2003) Transient calretinin expression defines early postmitotic step of neuronal differentiation in adult hippocampal neurogenesis of mice. Mol Cell Neurosci 24(3):603-613. doi: 10.1016/S1044-7431(03)00207-0.
43. Sloviter RS (1989) Calcium-binding protein (calbindin-D28k) and parvalbumin immunocytochemistry: localization in the rat hippocampus with specific reference to the selective vulnerability of hippocampal neurons to seizure activity. J Comp Neurol 280(2):183-196. doi: 10.1002/cne.902800203.
44. Sholl DA (1953) Dendritic organization in the neurons of the visual and motor cortices of the cat. J Anat 87(4):387-406.
45. Gavalda N, Gutierrez H, Davies AM (2009) Developmental switch in NF-kappaB signalling required for neurite growth. Development 136(20):3405-3412. doi: 10.1242/dev.035295.

46. Colao A, Ferone D, Marzullo P, Lombardi G (2004) Systemic complications of acromegaly: epidemiology, pathogenesis, and management. Endocr Rev 25(1):102–152. doi: 10.1210/er.2002-0022.

47. Deijen, JB, de Boer H, van der Veen EA (1998) Cognitive changes during growth hormone replacement in adult men. Psychoneuroendocrinology 23(1):45-55. doi: http://dx.doi.org/10.1016/S0306-4530(97)00092-9.

48. Schneider-Rivas S, Rivas Arancibia S, Vázquez-Pereyra F, Vázquez-Sandoval R, Borgonio-Pérez G (1995) Modulation of long-term memory and extinction responses induced by growth hormone (GH) and growth hormone releasing hormone (GHRH) in rats. Life Sci 56, PL433–PL441. 10.1016/0024-3205(95)00171-2.

49. Dyer AH, Vahdatpour C, Sanfeliu A, Tropea D. (2016). The role of Insulin-Like Growth Factor 1 (IGF-1) in brain development, maturation and neuroplasticity.Neuroscience 325:89-99. doi: 10.1016/j.neuroscience.2016.03.056

50. Basu A, McFarlane HG, Kopchick JJ (2017) Spatial learning and memory in male mice with altered growth hormone action. Horm Behav 93:18-30. doi: 10.1016/j.yhbeh.2017.04.001.

51. Balu DT, Lucki I (2009) Adult hippocampal neurogenesis: regulation, functional implications, and contribution to disease pathology. Neurosci Biobehav Rev 33(3):232-352. doi: 10.1016/j.neubiorev.2008.08.007.

52. Hashimotodani Y, Nasrallah K, Jensen KR, Chávez AE, Carrera D, Castillo PE (2017) LTP at Hilar Mossy Cell-Dentate Granule Cell Synapses Modulates Dentate Gyrus Output by Increasing Excitation/Inhibition Balance. Neuron 95(4):928-943. doi: 10.1016/j.neuron.2017.07.028.

53. Deng W, Aimone JB, Gage FH (2010) New neurons and new memories: how does adult hippocampal neurogenesis affect learning and memory? Nat Rev Neurosci 11(5):339-350. doi: 10.1038/nrn2822.

54. Bruel-Jungerman E, Davis S, Rampon C, Laroche S (2006) Long-term potentiation enhances neurogenesis in the adult dentate gyrus. J Neurosci 26(22):5888-5893. doi: 10.1523/JNEUROSCI.0782-06.2006.

55. van Praag H, Schinder AF, Christie BR, Toni N, Palmer TD, Gage FH (2002) Functional neurogenesis in the adult hippocampus. Nature 415(6875):1030-1034. doi: 10.1038/4151030a.

56. Karl C, Couillard-Despres S, Prang P, Munding M, Kilb W, Brigadski T, Plötz S, Mages W, Luhmann H, Winkler J, Bogdahn U, Aigner L (2005) Neuronal precursor-specific activity of a human doublecortin regulatory sequence. J Neurochem 92(2):264-282. doi: 10.1111/j.1471-4159.2004.02879.x.

57. Arruda-Carvalho M, Sakaguchi M, Akers KG, Josselyn SA, Frankland PW (2011) Posttraining ablation of adult-generated neurons degrades previously acquired memories. J Neurosci 31(42):15113-15127. doi: 10.1523/JNEUROSCI.3432-11.2011.

58. Devesa P, Agasse F, Xapelli S, Almengló C, Devesa J1, Malva JO, Arce VM (2014) Growth hormone pathways signaling for cell proliferation and survival in hippocampal neural precursors from postnatal mice. BMC Neurosci 15:100. doi: 10.1186/1471-2202-15-100.

59. Sievers C, Sämann PG, Dose T, Dimopoulou C, Spieler D, Roemmler J, Schopohl J, Mueller M, Schneider HJ, Czisch M, Pfister H, Stalla GK (2009) Macroscopic brain architecture changes and white matter pathology in acromegaly: a clinicoradiological study. Pituitary 12(3):177-85. doi: 10.1007/s11102-008-0143-1.

60. D'Ercole AJ, Ye P, O'Kusky JR (2002) Mutant mouse models of insulin-like growth factor actions in the central nervous system. Neuropeptides 36(2-3):209-20. doi: 10.1054/npep.2002.0893.

61. Van der Lely AJ, Beckers A, Daly AF, Lamberts SWJ, Clemmons DR (2005) Acromegaly: pathology, diagnosis and treatment. Boca Raton: Taylor & Francis.

62. Paxinos G, Watson C (1998) The rat brain in stereotaxic coordinates. San Diego, CA: Academic Press.

63. Wojtowicz JM, Kee N (2006) BrdU assay for neurogenesis in rodents. Nat Protoc 1(3):1399-1405. doi: 10.1038/nprot.2006.224.

64. Rao MS, Shetty AK (2004) Efficacy of doublecortin as a marker to analyse the absolute number and dendritic growth of newly generated neurons in the adult

dentate gyrus. Eur J Neurosci 19(2):234-246. doi: 10.1111/j.0953-816X.2003.03123.x.

65. Bayram-Weston Z, Olsen E, Harrison DJ, Dunnett SB, Brooks SP (2016) Optimising Golgi–Cox staining for use with perfusion-fixed brain tissue validated in the zQ175 mouse model of Huntington's disease. J Neurosci Methods 265:81–88. doi: 10.1016/j.jneumeth.2015.09.033.
66. Benjamini Y, Hochberg Y (1995) Controlling the false discovery rate: a practical and powerful approach to multiple testing. J R Statist Soc B 57(1): 289-300. doi:10.2307/2346101.
67. Contestabile A, Greco B, Ghezzi D, Tucci V, Benfenati F, Gasparini L (2013) Lithium rescues synaptic plasticity and memory in Down syndrome mice. J Clin Invest 123(1): 348–361. doi: 10.1172/JCI64650.

Tables

Table 1. List of primary antibodies used

Antibody	Dilution	Species	Staining	Source (Reference)
Anti-BrdU	1:200	Rat	IF, IHC	AbD Serotec (MCA2060)
Anti-DCX	1:250	Goat	IF, IHC	Santa Cruz (sc-8066)
Anti-NeuN	1:1000	Rabbit	IF	Millipore (ABN78)
Anti-Calretinin	1:2000	Rabbit	IF	Swant (7697)
Anti- Calbindin D-28k	1:2000	Rabbit	IF	Swant (CB-38a)
Anti-BM28 (MCM2)	1:500	Mouse	IF	BD Transduction (610701)

Figure legends

Figure 1. Experimental design. (**a**) Animals were divided in three experimental groups. Control rats (white square and bars) were injected in the right flank with vehicle and did not develop a tumor. Tumor-resected rats (blue square and bars) were injected in the right flank with a solution containing GC-cells and developed a tumor which was resected 8 weeks after the inoculation. And tumor-bearing rats (gray square and bars) were injected with GC cells in the right flank and consistently developed a tumor. Ten weeks after the injection, with either vehicle or GC cells, all animals were presented with different behavioral and electrophysiological tasks. (**b**) Rat weights measured the day of the inoculation of GC cells or vehicle (week 0, left set of bars), the day when the tumor was resected (week 8, middle set of bars), and the day of performing behavioral test (week 10, right set of bars). Note that tumor-bearing rats increased their body weight more than the control and tumor-resected animals. (**c**) Mean GH serum (s-GH) levels obtained by ELISA for: the control group, the tumor-resected group before (*B*) and after (*A*) tumor removal, and the tumor-bearing group the same day that the tumor was resected in the tumor-resected group (*B*), and days after (*A*). (**d**) Mean IGF-I serum (s-IGF-I) levels obtained by ELISA for the control group, the tumor-resected group before (*B*) and after (*A*) tumor removal, and the tumor-bearing group on the day that the tumor was resected in the tumor-resected group (*B*), and days after (*A*). Data are presented as mean ± SEM. †, $P < 0.01$; ‡, $P < 0.001$. *P* values were determined by one-way ANOVA with Tukey's post hoc test. †, $P < 0.01$; ‡, $P < 0.001$. *P* values were determined by two-way ANOVA repeated measures test followed by the Tukey HSD test.

Figure 2. Locomotion and exploration were not affected by the presence of the GH/IGF-I hypersecreting tumor. (**a**) Diagram of the open-field chamber. Rats locomotion was quantified as the number of times infrared photocells were interrupted in 15 min. (**b**) Total activity in the open-field during 15 min for control (n = 7), tumor-resected (n = 5) and tumor-bearing (n = 7) rats. The group factor did not reach significant differences ($P = 0.459$).

Figure 3. Chronic GH/IGF-I hypersecretion potentiated the acquisition of an operant conditioning task in behaving rats. (**a**) Rats (n = 5 per group) were trained in Skinner boxes to press a lever once to obtain a food pellet (FR 1:1 schedule). Afterward, they had to acquire an FR 5:1 schedule, in which they had to press the lever 5 times to obtain one pellet. (**b**) All groups acquired the FR 1:1 schedule with no statistical differences between them (BL, baseline; $P = 0.954$). Tumor-bearing rats performed the FR 5:1 schedule better than control and tumor-resected groups, pressing the lever significantly more times than the other two experimental groups ($P \leq 0.04$). (**c**) Animals were later transferred to a light/dark paradigm following an FR 5:1 in which lever presses were reinforced only when a small light bulb was switched on. A light on/off coefficient was computed as the difference between the numbers of lever presses when the light was on and when the light was off, divided by the total lever presses. (**d**) The tumor-bearing group always performed a higher number of lever presses when the light was on than did the control and the tumor-resected groups ($P \leq 0.038$). *, $P < 0.05$; †, $P < 0.01$; ‡, $P < 0.001$.

Figure 4. Chronic GH/IGF-I hypersecretion improved long-term passive avoidance memories in behaving rats. (**a**) For the passive avoidance test, the chamber was divided into a lit compartment and a dark compartment, with a gate between them. Animals were placed initially in the lit, stressful compartment. After 30 s, the gate opened, and the rat could enter the dark, stress-relieving compartment, where it received a mild foot shock (baseline). At 24 h, 72 h, and 1 week after the foot shock, rats were reintroduced into the light-dark box, and the time for rats to enter the dark compartment (latency to step-through) was measured. (**b**) During baseline recordings all the animals (n = 5 per group) entered the dark compartment within short periods of time, with no statistical differences between them ($P \geq 0.519$). At 24 h after receiving the foot shock, all groups avoided entering the dark compartment, since they remembered where they had received the foot shock ($P \geq 1.0$). Interestingly, only the tumor-bearing group avoided entering the dark compartment 72 h and 1 week after the baseline, while the other groups, saline-injected and tumor-resected, significantly reduced their latency to step-through. ‡, $P < 0.001$.

Figure 5. Chronic GH/IGF-I hypersecretion enhances long-term potentiation in behaving rats. (**a**) Animals were implanted with stimulating electrodes at Schaffer collaterals and with a recording tetrode in the CA1 area. To evoke LTP, animals were stimulated with the HFS protocol described in Methods. (**b**) Superimposed representative fEPSPs collected from control, tumor-resected and tumor-bearing rats before (baseline, B) and after (1, 2) HFS. (**c**) Time course of LTP following HFS. The HFS was presented after 15 min of baseline recording, at the time marked by the dashed line. Changes in fEPSP amplitudes were quantified as percentage of baseline (100%) values. The fEPSP amplitudes of tumor-bearing rats were significantly ($P \leq 0.024$) larger than those of control and tumor-resected groups during the four days of recording. N = 12 rats per group. *, $P < 0.05$; †, $P < 0.01$; ‡, $P < 0.001$.

Figure 6. Chronic GH/IGF-I hypersecretion did not increase adult hippocampal neurogenesis but promoted neuronal differentiation (**a**) At week 10, the three experimental groups were injected with BrdU for three consecutive days. All animals were perfused 4 h after the last injection. (**b**) Schematic diagram of the sequential process of adult hippocampal neurogenesis occurring in the subgranular zone of the hippocampus. The figure, adapted from (34,67), depicts markers used in this study. An activated radial glia-like progenitor passes through distinct phases as it differentiates, matures, and functionally integrates with an elaborate morphology into the neuronal circuit. Each of the phases and the respective cell types were identified based on their expression of a combination of markers. The thymidine analogue 5′-bromodeoxyuridine (BrdU) is a proliferation marker, which incorporates into the DNA of dividing cells during the S-phase of the cell cycle. MCM2 is a proliferation marker, which is expressed across all the mitotic progenitor cell types. In the post-mitotic progenitor (immature new-born neuron), MCM2 expression is lost, while doublecortin (DCX) expression dictates migration and maturation into a functional neuron. (**c**) Immunochemistry of BrdU, DCX, and MCM2/DCX in the subgranular zone of control, tumor-resected and tumor-bearing groups. Right column shows, from top to bottom, densities of BrdU, DCX, and MCM2/DCX immunopositive

cells in the subgranular zone of the dentate gyrus of control (n = 6), tumor-resected (n = 5), and tumor-bearing (n = 7) rats. Scale bars = 50 μm. *, $P < 0.05$.

Figure 7. Chronic GH/IGF-I hypersecretion promotes neuronal migration and maturation (**a**) At week 10, the three groups were injected with BrdU for three consecutive days. All animals were perfused 3 weeks after the last injection. (**b**) Same diagram as in Figure 6a. Immature neurons migrate over a short distance to reach the granular layer of the dentate gyrus. The immature and postmitotic neurons extend their axons toward the pyramidal layer of the hippocampal area CA3 and send their dendrites in the direction of the molecular layer of the dentate gyrus. The new granule cells are synaptically integrated into the network of the hippocampal formation, receiving inputs from the entorhinal cortex and sending outputs to the hippocampal area CA3 and the hilus. NeuN is used as a marker of postmitotic cells, and labels both "normal" and newly-generated postmitotic neurons. Calretinin (CR) is the marker for immature postmitotic neurons ─ its expression within the dentate gyrus is restricted to a short postmitotic time-window in which axonal and dendritic targeting is assumed to take place. Calbindin (CB) is used as a marker for mature granule cells, since it is expressed in mature neurons together with NeuN but is not co-expressed with calretinin. (**c**) Newly generated hippocampal granule neurons, as detected 21 days after BrdU injection. Newborn neurons were identified by BrdU and NeuN, CR, or CB immunostaining. For each group, the left column displays representative images for cells showing double labeling in the subgranular zone, 21 days after BrdU injection. Quantitative data are expressed as the mean number of double-positive cells per section. The number of mature neurons incorporated in the dentate gyrus during the BrdU differentiation assay was significantly increased in the tumor-bearing group (gray square, gray bar), which mainly colocalized with NeuN and CB; n = 4 per group. *, $P < 0.05$; ‡, $P < 0.001$.

Figure 8. Chronic GH/IGF-I hypersecretion enhances complexity of dendritic arbors and increases dendritic spine density on hippocampal granule neurons. The complexity of dendritic arbors was assessed using Sholl analysis to determine the number of dendritic intersections crossing equidistant concentric circles. (**a**) Drawings and photomicrographs of

representative neurons from control, tumor-resected, and tumor-bearing groups labeled with doublecortin (DCX). Scale bars = 50 μm. (**b**) Quantification of the number of dendritic intersections per circle. Significant differences were found for circles ranging from 60 μm to 100 μm in the tumor-bearing group compared with tumor-resected and control groups. (**c**) Quantification of the maximum dendritic length in the dentate gyrus. (**d**) Quantification of total neurite length of DCX-positive neurons in the dentate gyrus. (**e**) Golgi-Cox staining was performed to quantify the spine density in each experimental group. Representative high-magnification images of Golgi-Cox staining of hippocampal sections from control, tumor-resected, and tumor-bearing groups. Scale bars = 5 μm. (**f**) Quantification of dendritic spine density. Results are shown as mean ± SEM of spine number per 10 μm dendritic length (12 neurons/rat and 3 rats/group). Note that newly born neurons from the tumor-bearing group exhibit an increased dendritic spine number as compared with the other two groups. *, $P < 0.05$; †, $P < 0.01$.

Figure 1

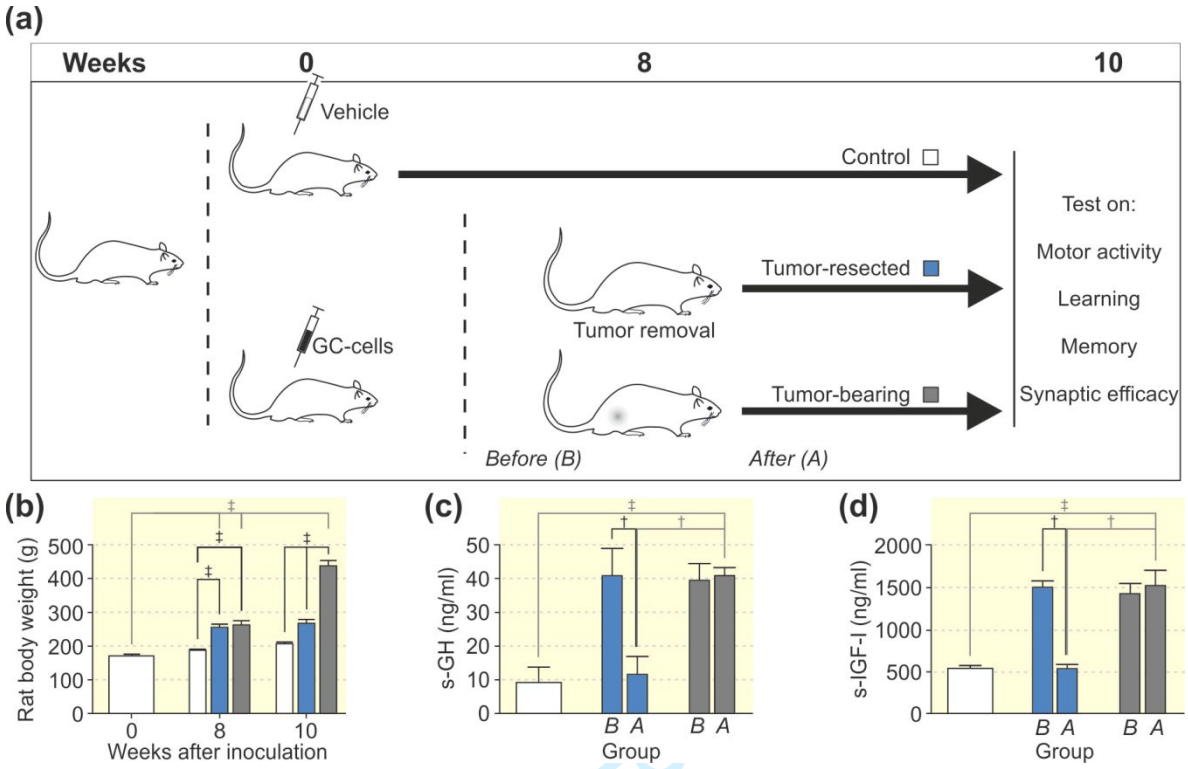

Figure 2

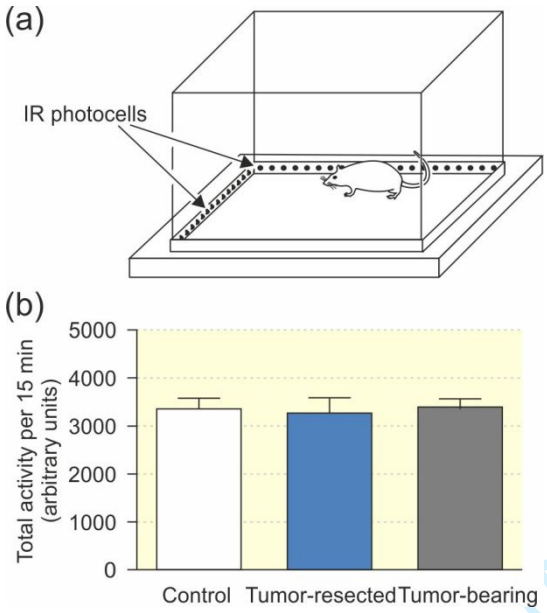

Figure 3

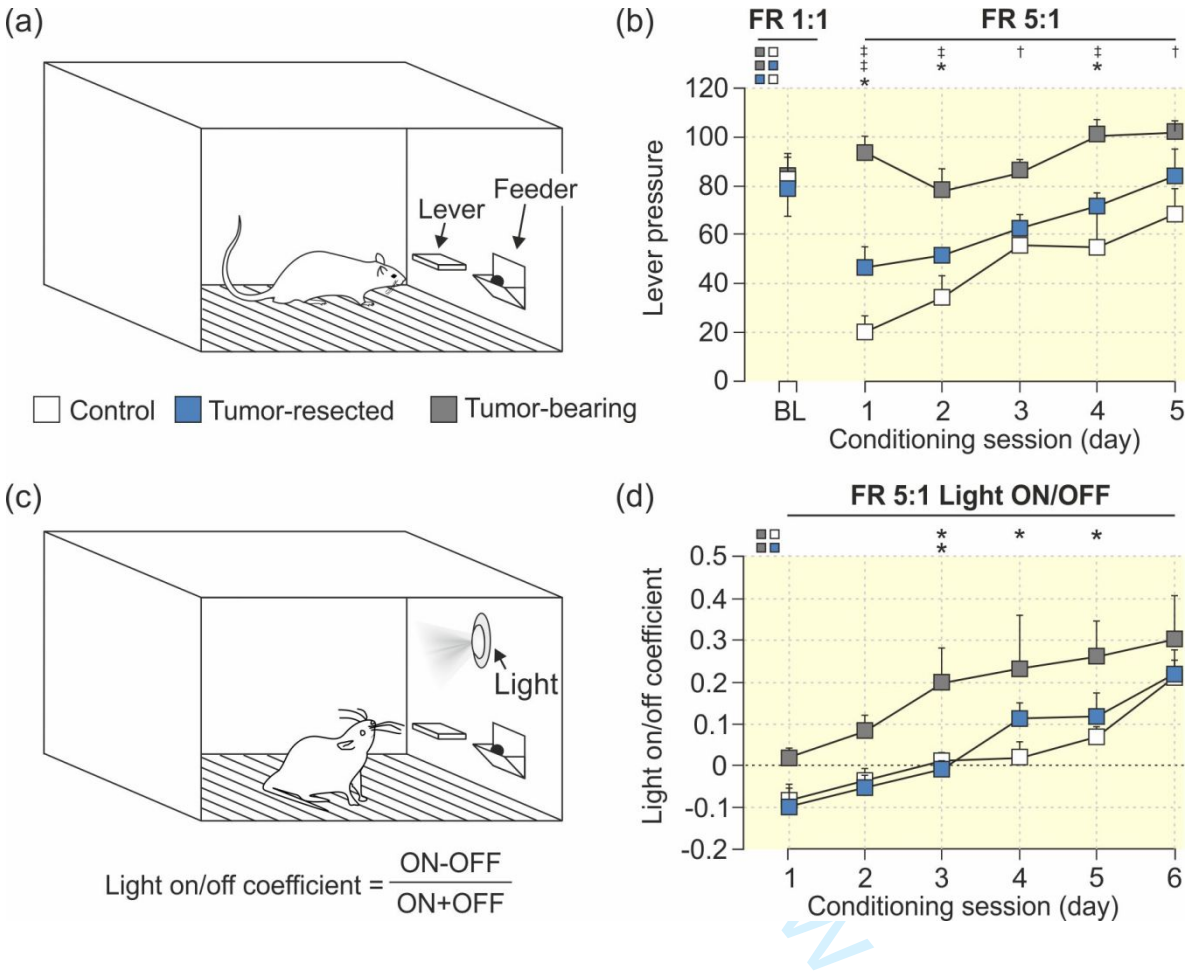
(a)
Lever
Feeder
Control
Tumor-resected
Tumor-bearing
(b)
FR 1:1
FR 5:1
Lever pressure
120
100
80
60
40
20
0
BL
1
2
3
4
5
Conditioning session (day)
(c)
Light
Light on/off coefficient = ON-OFF / ON+OFF
(d)
FR 5:1 Light ON/OFF
Light on/off coefficient
0.5
0.4
0.3
0.2
0.1
0
-0.1
-0.2
1
2
3
4
5
6
Conditioning session (day)

Figure 4

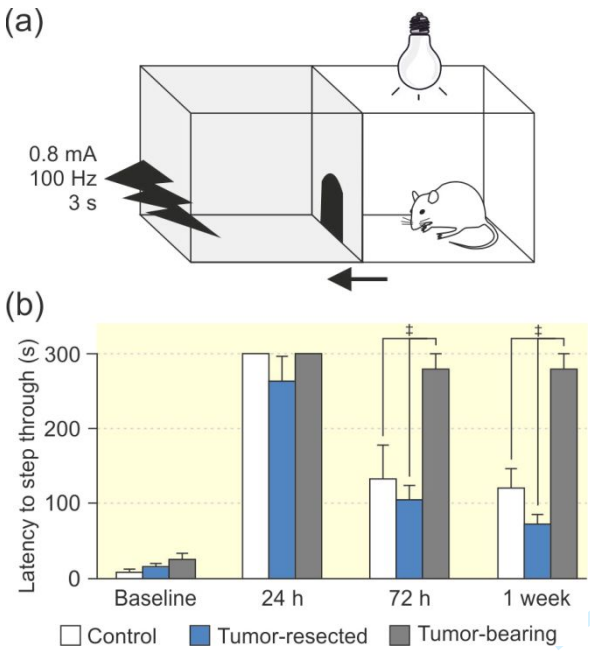

Figure 5

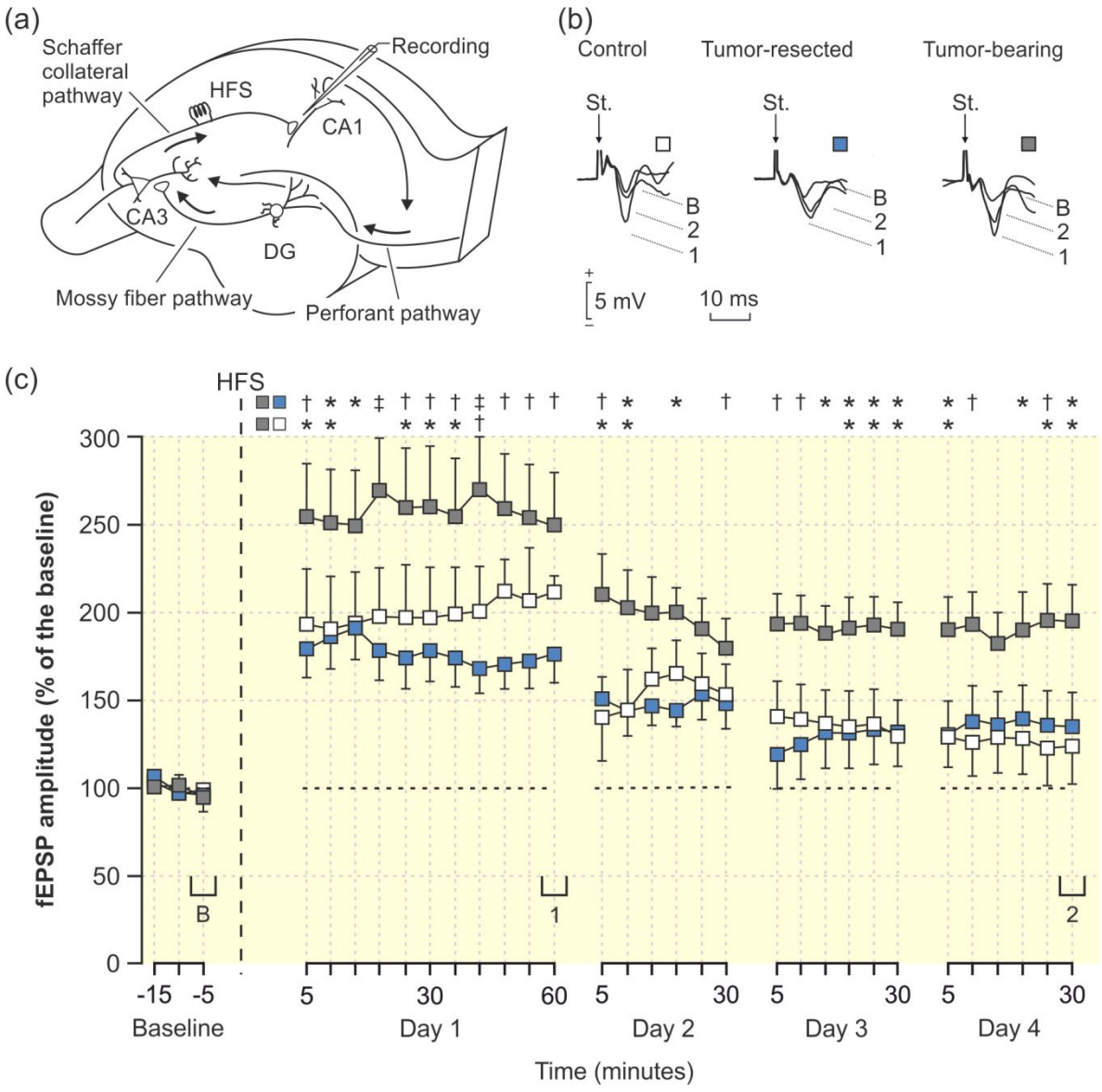
(a)
Schaffer collateral pathway
HFS
Recording
CA1
CA3
DG
Mossy fiber pathway
Perforant pathway
(b)
Control
Tumor-resected
Tumor-bearing
St.
B
2
1
5 mV
10 ms
(c)
HFS
fEPSP amplitude (% of the baseline)
300
250
200
150
100
50
0
B
1
2
-15
-5
5
30
60
Baseline
Day 1
Day 2
Day 3
Day 4
Time (minutes)

Figure 6

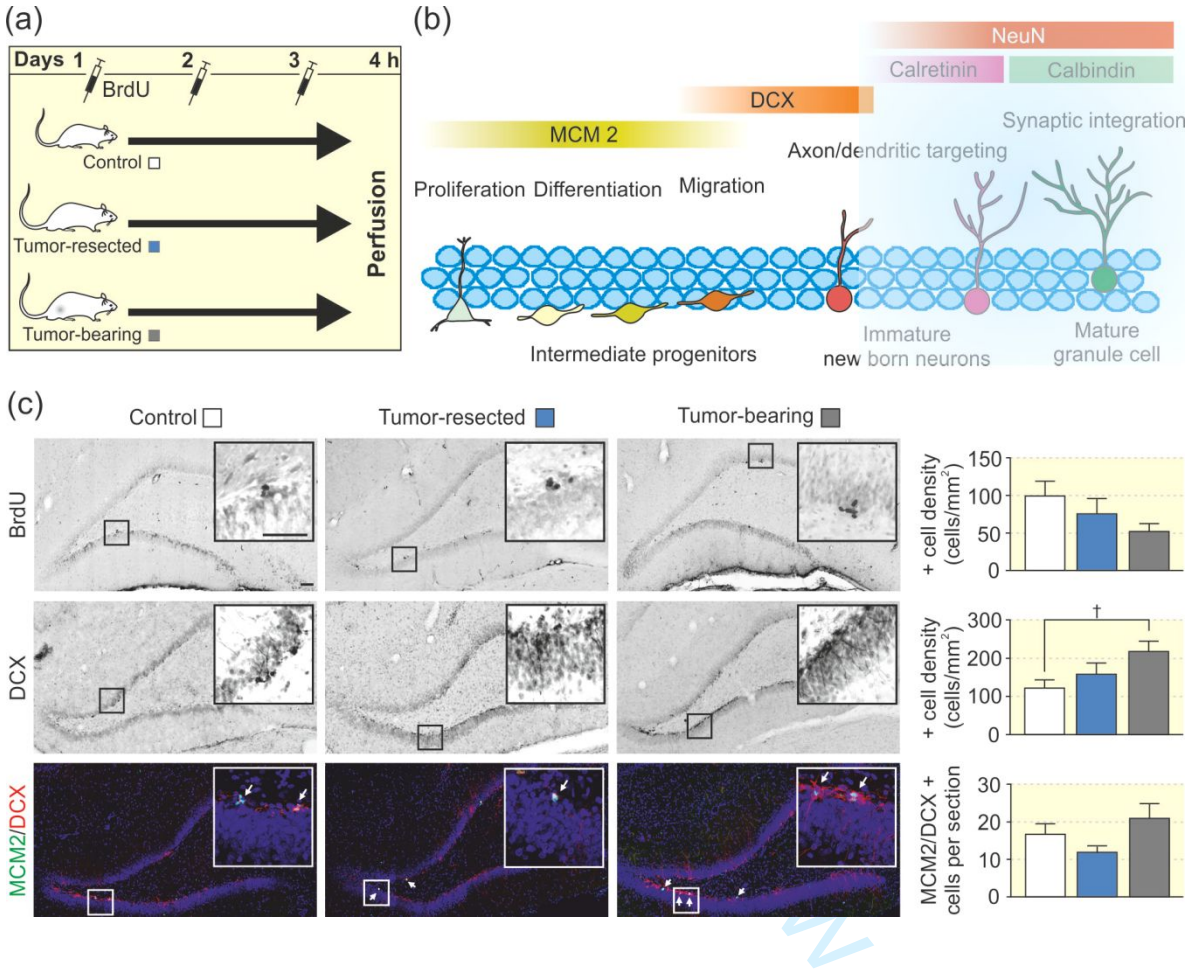
(a)
Days 1
2
3
4 h
BrdU
Control
Tumor-resected
Tumor-bearing
Perfusion
(b)
NeuN
Calretinin
Calbindin
DCX
MCM 2
Synaptic integration
Axon/dendritic targeting
Proliferation
Differentiation
Migration
Intermediate progenitors
Immature new born neurons
Mature granule cell
(c)
Control
Tumor-resected
Tumor-bearing
BrdU
DCX
MCM2/DCX
+ cell density (cells/mm²)
150
100
50
0
300
200
100
0
†
MCM2/DCX + cells per section
30
20
10
0

Figure 7

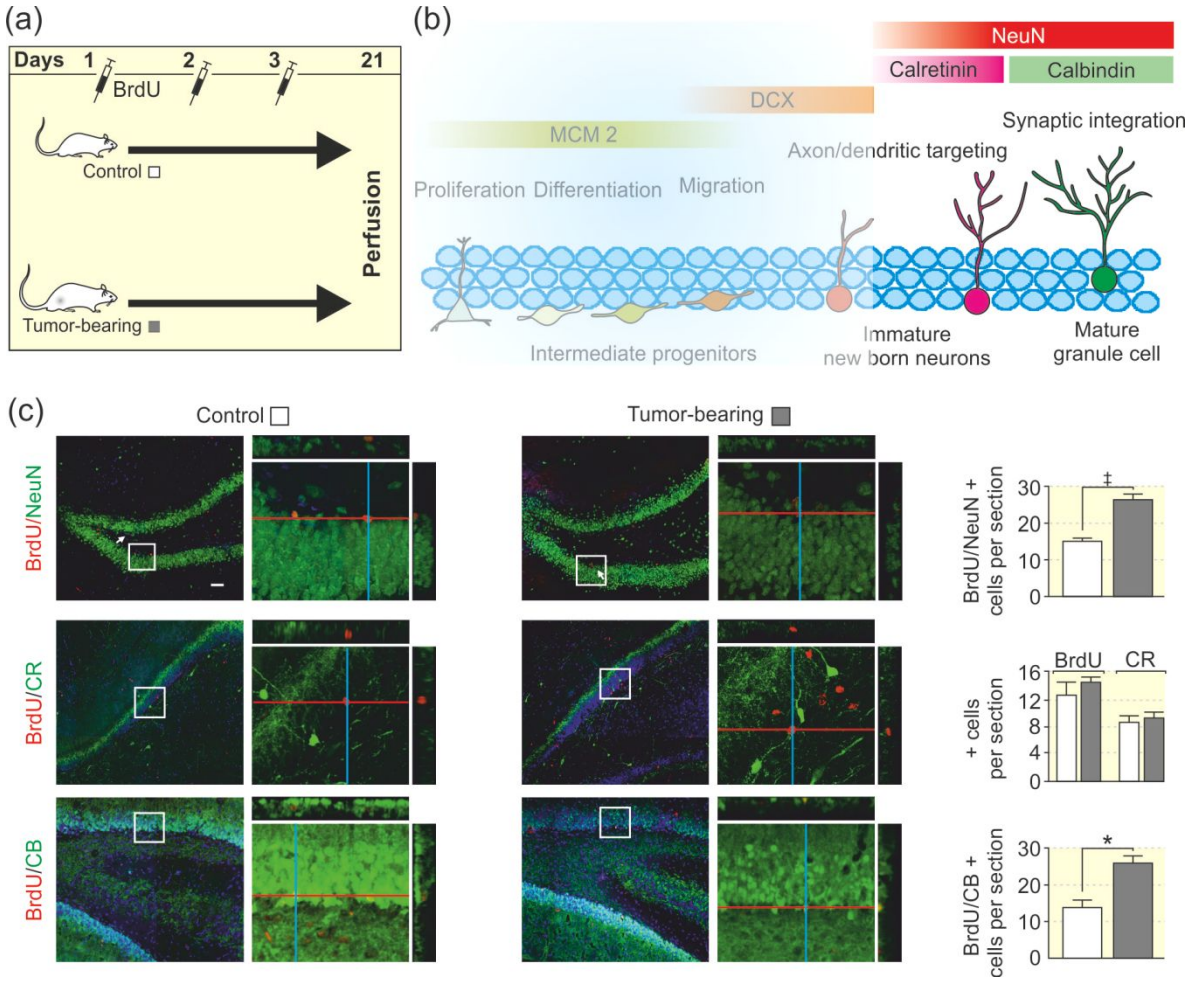
(a)
Days 1 2 3 21
BrdU
Control
Tumor-bearing
Perfusion
(b)
NeuN
Calretinin
Calbindin
DCX
MCM 2
Synaptic integration
Axon/dendritic targeting
Proliferation Differentiation Migration
Intermediate progenitors
Immature new born neurons
Mature granule cell
(c)
Control
Tumor-bearing
BrdU/NeuN
BrdU/CR
BrdU/CB
BrdU/NeuN + cells per section
BrdU
CR
+ cells per section
BrdU/CB + cells per section

Figure 8

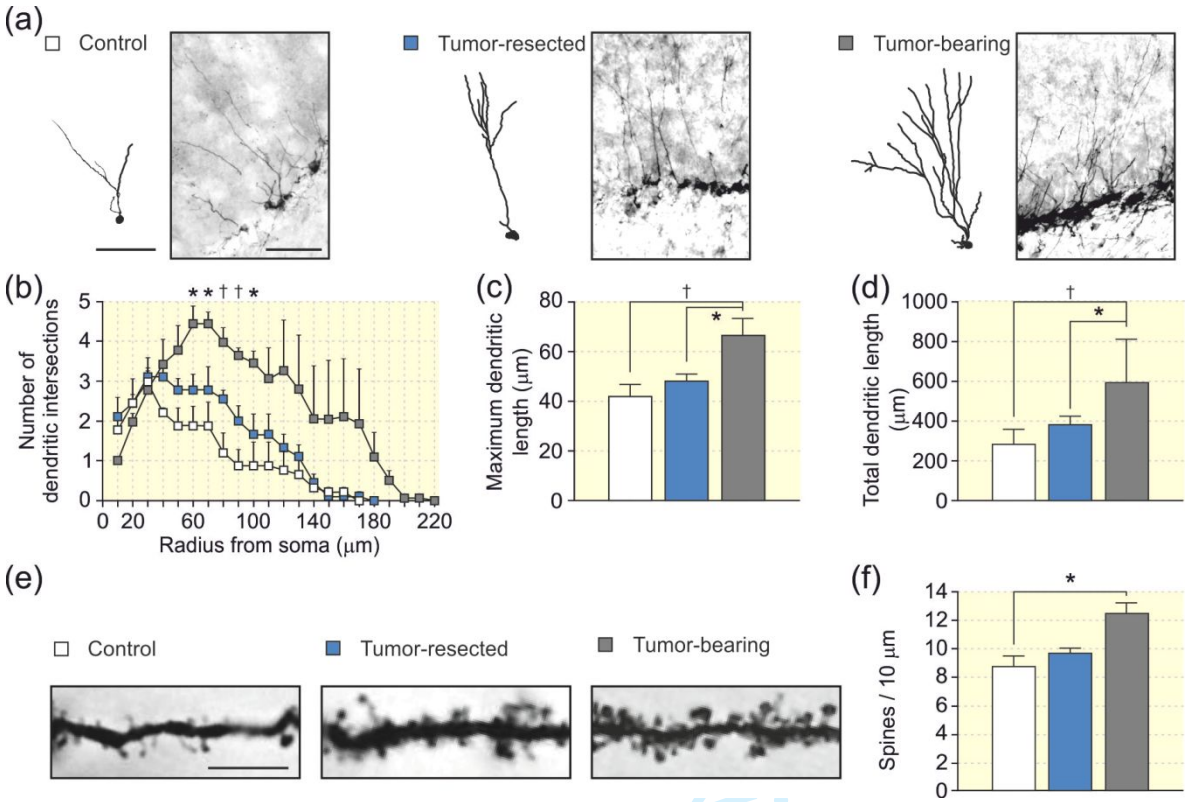

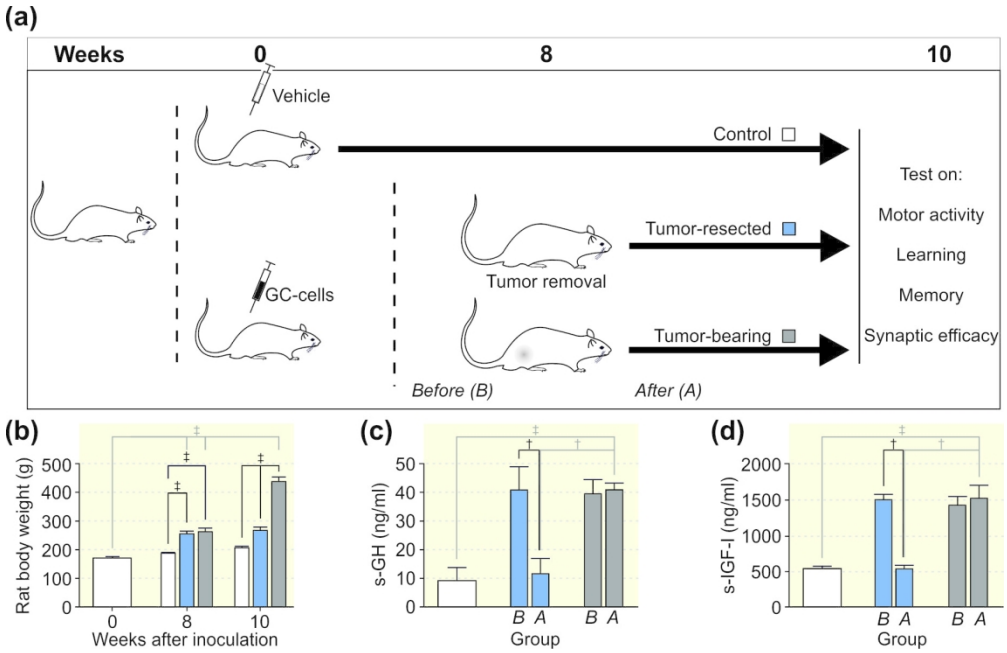

Figure 1. Experimental design. (a) Animals were divided in three experimental groups. Control rats (white square and bars) were injected in the right flank with vehicle and did not develop a tumor. Tumor-resected rats (blue square and bars) were injected in the right flank with a solution containing GC-cells and developed a tumor which was resected 8 weeks after the inoculation. And tumor-bearing rats (gray square and bars) were injected with GC cells in the right flank and consistently developed a tumor. Ten weeks after the injection, with either vehicle or GC cells, all animals were presented with different behavioral and electrophysiological tasks. (b) Rat weights measured the day of the inoculation of GC cells or vehicle (week 0, left set of bars), the day when the tumor was resected (week 8, middle set of bars), and the day of performing behavioral test (week 10, right set of bars). Note that tumor-bearing rats increased their body weight more than the control and tumor-resected animals. (c) Mean GH serum (s-GH) levels obtained by ELISA for: the control group, the tumor-resected group before (B) and after (A) tumor removal, and the tumor-bearing group the same day that the tumor was resected in the tumor-resected group (B), and days after (A). (d) Mean IGF-I serum (s-IGF-I) levels obtained by ELISA for the control group, the tumor-resected group before (B) and after (A) tumor removal, and the tumor-bearing group on the day that the tumor was resected in the tumor-resected group (B), and days after (A). Data are presented as mean ± SEM. †, $P < 0.01$; ‡, $P < 0.001$. P values were determined by one-way ANOVA with Tukey's post hoc test. †, $P < 0.01$; ‡, $P < 0.001$. P values were determined by two-way ANOVA repeated measures test followed by the Tukey HSD test.

157x100mm (300 x 300 DPI)

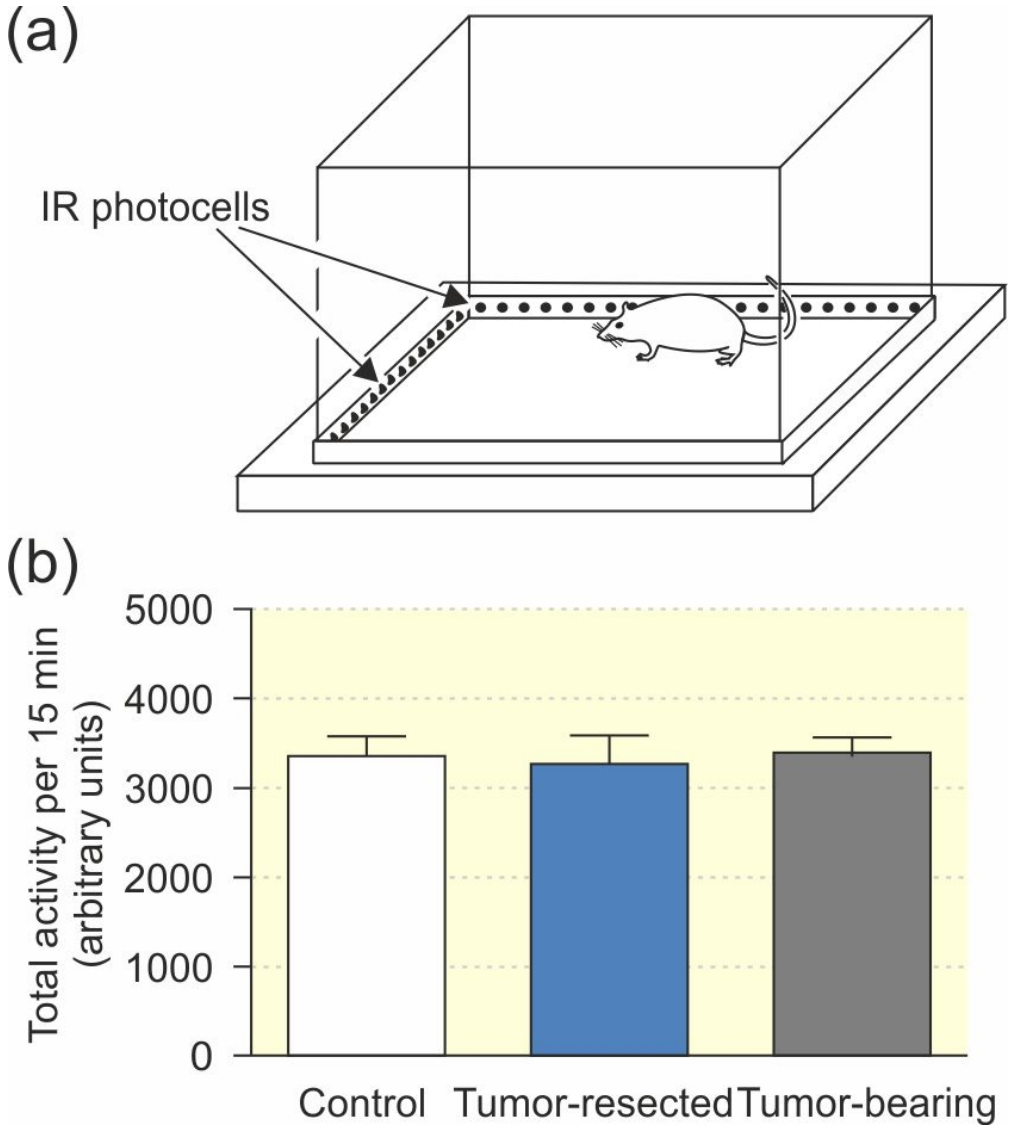

Figure 2. Locomotion and exploration were not affected by the presence of the GH/IGF-I hypersecreting tumor. (a) Diagram of the open-field chamber. Rats locomotion was quantified as the number of times infrared photocells were interrupted in 15 min. (b) Total activity in the open-field during 15 min for control (n = 7), tumor-resected (n = 5) and tumor-bearing (n = 7) rats. The group factor did not reach significant differences (P = 0.459).

71x79mm (300 x 300 DPI)

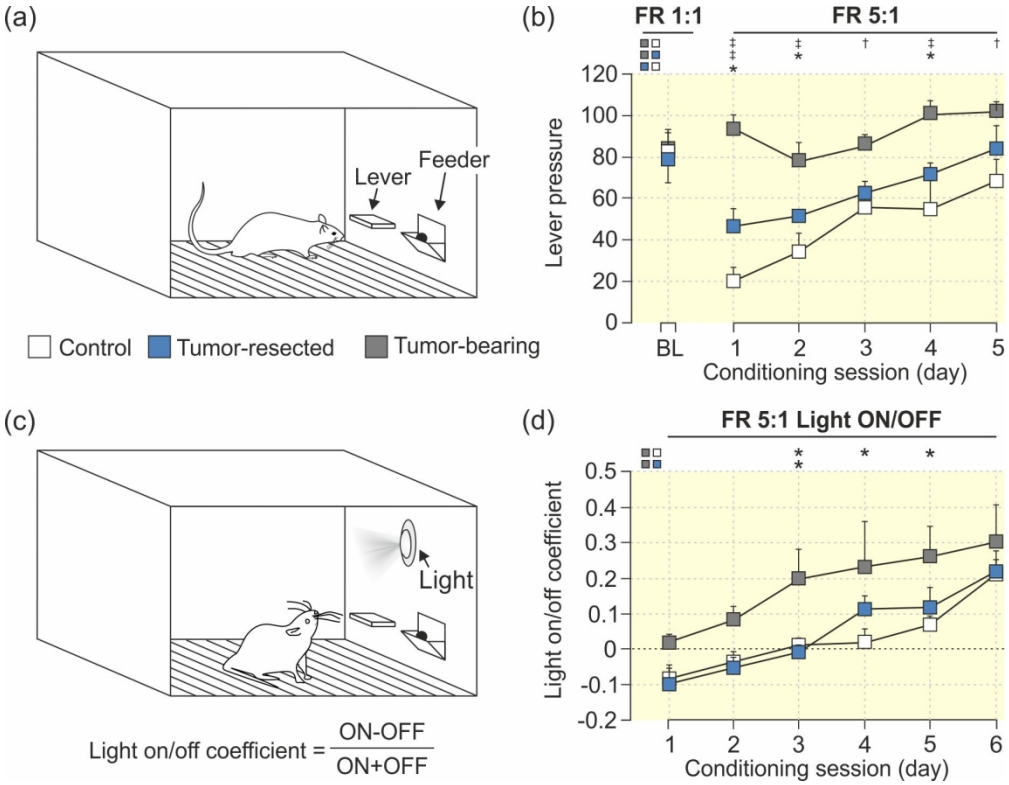

Figure 3. Chronic GH/IGF-I hypersecretion potentiated the acquisition of an operant conditioning task in behaving rats. (a) Rats (n = 5 per group) were trained in Skinner boxes to press a lever once to obtain a food pellet (FR 1:1 schedule). Afterward, they had to acquire an FR 5:1 schedule, in which they had to press the lever 5 times to obtain one pellet. (b) All groups acquired the FR 1:1 schedule with no statistical differences between them (BL, baseline; $P = 0.954$). Tumor-bearing rats performed the FR 5:1 schedule better than control and tumor-resected groups, pressing the lever significantly more times than the other two experimental groups ($P \leq 0.04$). (c) Animals were later transferred to a light/dark paradigm following an FR 5:1 in which lever presses were reinforced only when a small light bulb was switched on. A light on/off coefficient was computed as the difference between the numbers of lever presses when the light was on and when the light was off, divided by the total lever presses. (d) The tumor-bearing group always performed a higher number of lever presses when the light was on than did the control and the tumor-resected groups ($P \leq 0.038$). *, $P < 0.05$; †, $P < 0.01$; ‡, $P < 0.001$.

157x122mm (300 x 300 DPI)

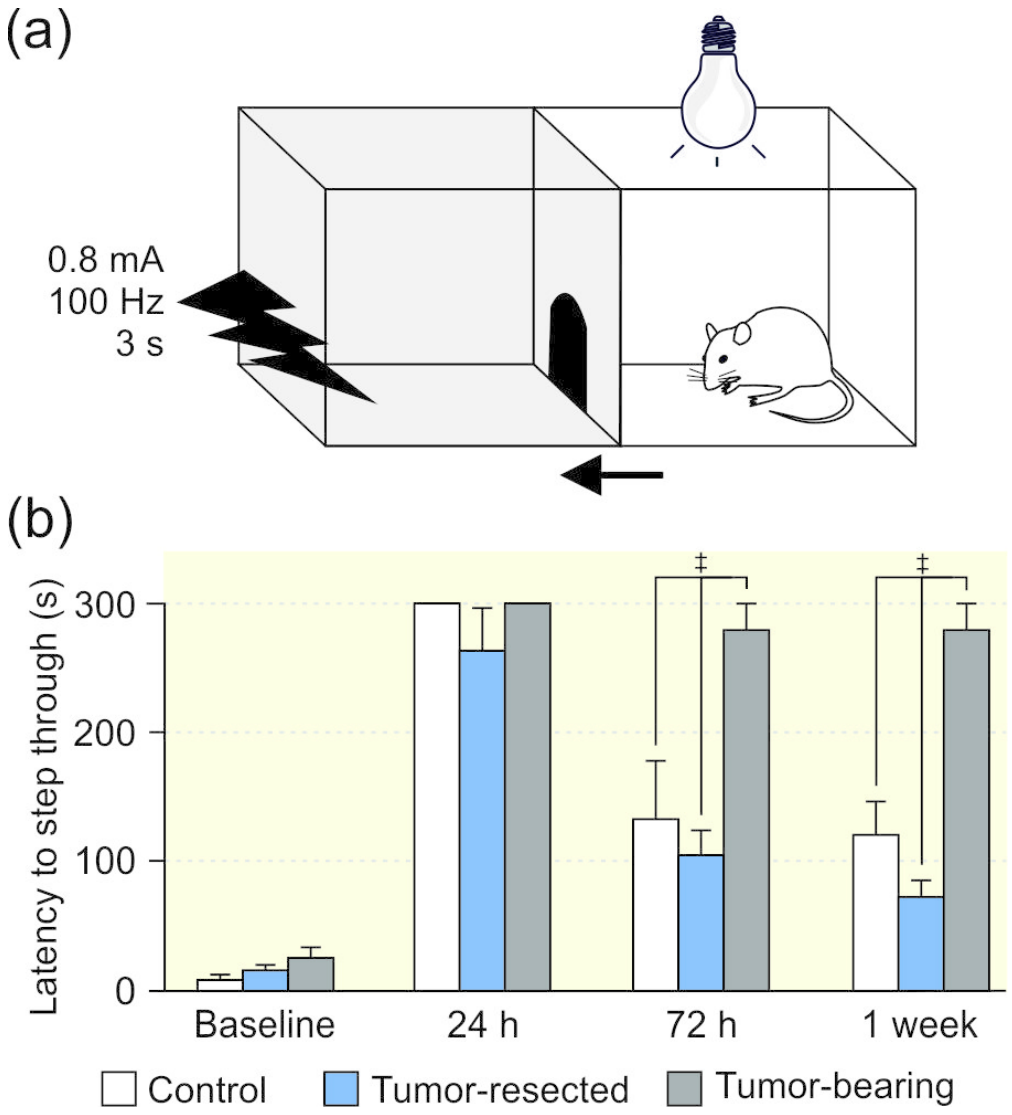

Figure 4. Chronic GH/IGF-I hypersecretion improved long-term passive avoidance memories in behaving rats. (a) For the passive avoidance test, the chamber was divided into a lit compartment and a dark compartment, with a gate between them. Animals were placed initially in the lit, stressful compartment. After 30 s, the gate opened, and the rat could enter the dark, stress-relieving compartment, where it received a mild foot shock (baseline). At 24 h, 72 h, and 1 week after the foot shock, rats were reintroduced into the light-dark box, and the time for rats to enter the dark compartment (latency to step-through) was measured. (b) During baseline recordings all the animals (n = 5 per group) entered the dark compartment within short periods of time, with no statistical differences between them ($P \geq 0.519$). At 24 h after receiving the foot shock, all groups avoided entering the dark compartment, since they remembered where they had received the foot shock ($P \geq 1.0$). Interestingly, only the tumor-bearing group avoided entering the dark compartment 72 h and 1 week after the baseline, while the other groups, saline-injected and tumor-resected, significantly reduced their latency to step-through. ‡, $P < 0.001$.

76x84mm (300 x 300 DPI)

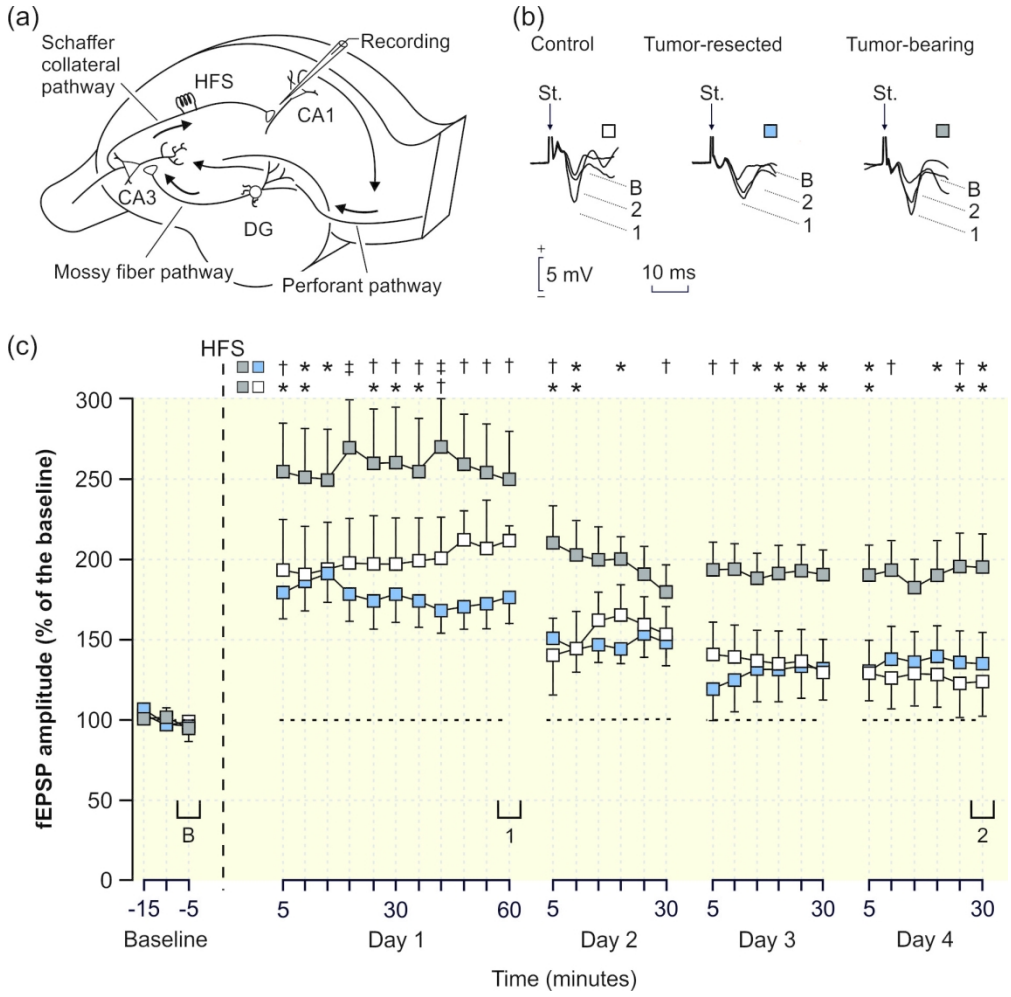

Figure 5. Chronic GH/IGF-I hypersecretion enhances long-term potentiation in behaving rats. (a) Animals were implanted with stimulating electrodes at Schaffer collaterals and with a recording tetrode in the CA1 area. To evoke LTP, animals were stimulated with the HFS protocol described in Methods. (b) Superimposed representative fEPSPs collected from control, tumor-resected and tumor-bearing rats before (baseline, B) and after (1, 2) HFS. (c) Time course of LTP following HFS. The HFS was presented after 15 min of baseline recording, at the time marked by the dashed line. Changes in fEPSP amplitudes were quantified as percentage of baseline (100%) values. The fEPSP amplitudes of tumor-bearing rats were significantly ($P \leq 0.024$) larger than those of control and tumor-resected groups during the four days of recording. N = 12 rats per group. *, $P < 0.05$; †, $P < 0.01$; ‡, $P < 0.001$.

161x158mm (300 x 300 DPI)

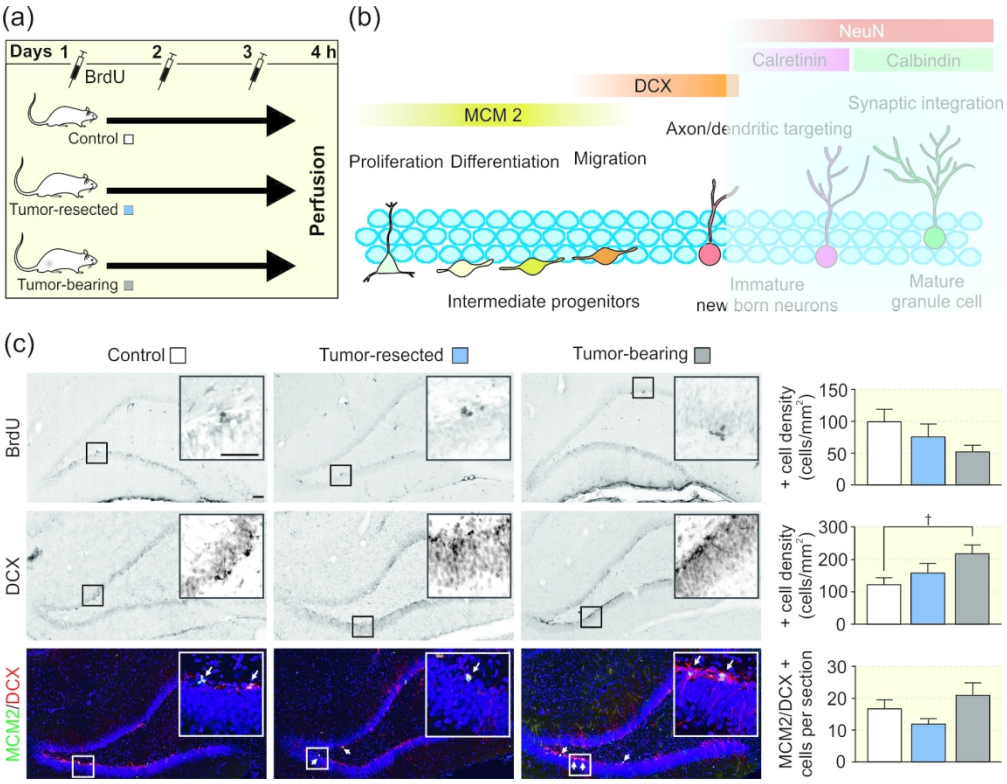

Figure 6. Chronic GH/IGF-I hypersecretion did not increase adult hippocampal neurogenesis but promoted neuronal differentiation (a) At week 10, the three experimental groups were injected with BrdU for three consecutive days. All animals were perfused 4 h after the last injection. (b) Schematic diagram of the sequential process of adult hippocampal neurogenesis occurring in the subgranular zone of the hippocampus. The figure, adapted from (34,67), depicts markers used in this study. An activated radial glia-like progenitor passes through distinct phases as it differentiates, matures, and functionally integrates with an elaborate morphology into the neuronal circuit. Each of the phases and the respective cell types were identified based on their expression of a combination of markers. The thymidine analogue 5′-bromodeoxyuridine (BrdU) is a proliferation marker, which incorporates into the DNA of dividing cells during the S-phase of the cell cycle. MCM2 is a proliferation marker, which is expressed across all the mitotic progenitor cell types. In the post-mitotic progenitor (immature new-born neuron), MCM2 expression is lost, while doublecortin (DCX) expression dictates migration and maturation into a functional neuron. (c) Immunochemistry of BrdU, DCX, and MCM2/DCX in the subgranular zone of control, tumor-resected and tumor-bearing groups. Right column shows, from top to bottom, densities of BrdU, DCX, and MCM2/DCX immunopositive cells in the subgranular zone of the dentate gyrus of control (n = 6), tumor-resected (n = 5), and tumor-bearing (n = 7) rats. Scale bars = 50 □m. *, P < 0.05.

159x123mm (300 x 300 DPI)

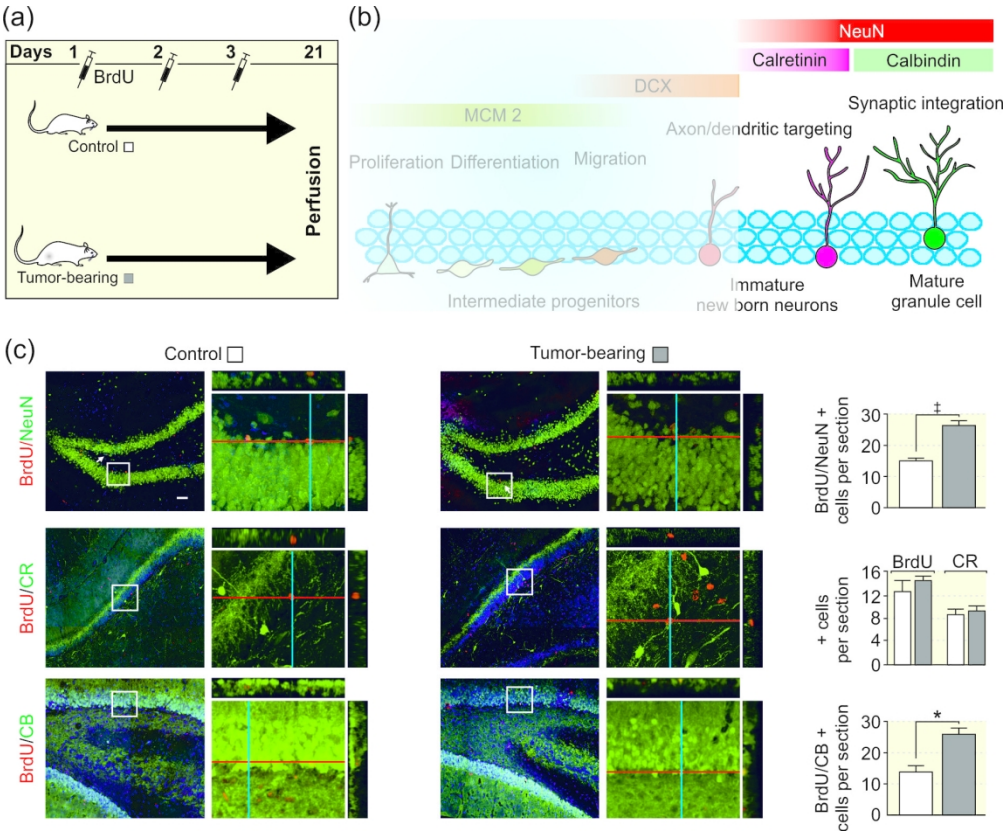

Figure 7. Chronic GH/IGF-I hypersecretion promotes neuronal migration and maturation (a) At week 10, the three groups were injected with BrdU for three consecutive days. All animals were perfused 3 weeks after the last injection. (b) Same diagram as in Figure 6a. Immature neurons migrate over a short distance to reach the granular layer of the dentate gyrus. The immature and postmitotic neurons extend their axons toward the pyramidal layer of the hippocampal area CA3 and send their dendrites in the direction of the molecular layer of the dentate gyrus. The new granule cells are synaptically integrated into the network of the hippocampal formation, receiving inputs from the entorhinal cortex and sending outputs to the hippocampal area CA3 and the hilus. NeuN is used as a marker of postmitotic cells, and labels both "normal" and newly-generated postmitotic neurons. Calretinin (CR) is the marker for immature postmitotic neurons — its expression within the dentate gyrus is restricted to a short postmitotic time-window in which axonal and dendritic targeting is assumed to take place. Calbindin (CB) is used as a marker for mature granule cells, since it is expressed in mature neurons together with NeuN but is not co-expressed with calretinin. (c) Newly generated hippocampal granule neurons, as detected 21 days after BrdU injection. Newborn neurons were identified by BrdU and NeuN, CR, or CB immunostaining. For each group, the left column displays representative images for cells showing double labeling in the subgranular zone, 21 days after BrdU injection. Quantitative data are expressed as the mean number of double-positive cells per section. The number of mature neurons incorporated in the dentate gyrus during the BrdU differentiation assay was significantly increased in the tumor-bearing group (gray square, gray bar), which mainly colocalized with NeuN and CB; n = 4 per group. *, $P < 0.05$; ‡, $P < 0.001$.

159x131mm (300 x 300 DPI)

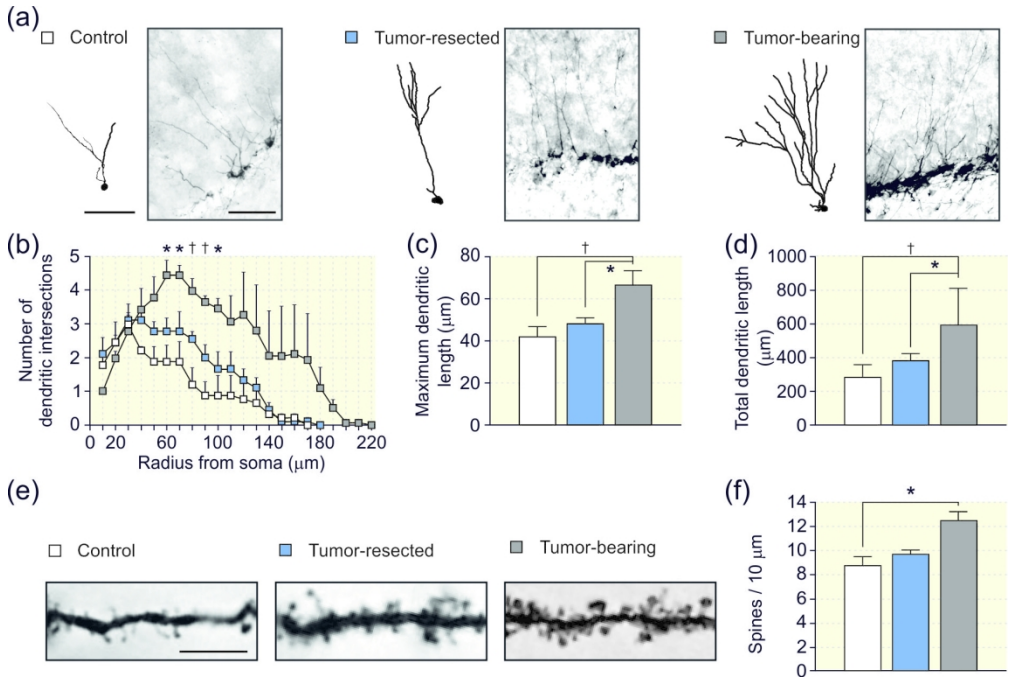

Figure 8. Chronic GH/IGF-I hypersecretion enhances complexity of dendritic arbors and increases dendritic spine density on hippocampal granule neurons. The complexity of dendritic arbors was assessed using Sholl analysis to determine the number of dendritic intersections crossing equidistant concentric circles. (a) Drawings and photomicrographs of representative neurons from control, tumor-resected, and tumor-bearing groups labeled with doublecortin (DCX). Scale bars = 50 μm. (b) Quantification of the number of dendritic intersections per circle. Significant differences were found for circles ranging from 60 μm to 100 μm in the tumor-bearing group compared with tumor-resected and control groups. (c) Quantification of the maximum dendritic length in the dentate gyrus. (d) Quantification of total neurite length of DCX-positive neurons in the dentate gyrus. (e) Golgi-Cox staining was performed to quantify the spine density in each experimental group. Representative high-magnification images of Golgi-Cox staining of hippocampal sections from control, tumor-resected, and tumor-bearing groups. Scale bars = 5 μm. (f) Quantification of dendritic spine density. Results are shown as mean ± SEM of spine number per 10 μm dendritic length (12 neurons/rat and 3 rats/group). Note that newly born neurons from the tumor-bearing group exhibit an increased dendritic spine number as compared with the other two groups. *, $P < 0.05$; †, $P < 0.01$.

158x106mm (300 x 300 DPI)